universität wien

MASTERARBEIT / MASTER'S THESIS

Titel der Masterarbeit / Title of the Master's Thesis

Linking the genetic potential for denitrification with physiological traits of ammonia-oxidizing bacteria

verfasst von / submitted by

Daniel Loy, BSc

angestrebter akademischer Grad / in partial fulfilment of the requirements for the degree of

Master of Science (MSc)

Wien, 2023 / Vienna, 2023

Studienkennzahl lt. Studienblatt / degree programme code as it appears on the student record sheet:	UA 066 830
Studienrichtung lt. Studienblatt / degree programme as it appears on the student record sheet:	Masterstudium Molecular Microbiology, Microbial Ecology and Immunobiology
Betreut von / Supervisor:	Univ.-Prof. Dipl.-Biol. Dr. Holger Daims

Table of Contents

SUMMARY

Nitrous oxide (N_2O) is a potent greenhouse gas produced by a variety of microorganisms, including ammonia-oxidizing bacteria (AOB). The enzymatic pathway for N_2O production in AOB involves the sequential reduction of nitrite (NO_2^-) to N_2O by two enzymes: nitrite reductase (NIR) and nitric oxide reductase (NOR). Two putative NORs have been identified in AOB. The cNOR is well known to be involved in nitric oxide (NO) reduction but the role of the sNOR is still unclear.

The main goal of this study was to investigate AOB with different genetic makeups to clarify the main contributors to N_2O production and the role of the sNOR. Three AOB strains all encoding a NIR (NirK), but with varying NOR compositions were utilized: *Nitrosomonas europaea* Nm50 (cNOR and sNOR), *Nitrosospira multiformis* Nl13 (no NORs), and *Nitrosospira briensis* Nsp1 (sNOR). A microrespiration system was used to simultaneously measure oxygen (O_2), NO, and N_2O in a closed glass chamber. This setup allowed for substrate injections at any time and real-time observations of all three gases.

The results showed that the sNOR does not seem to be involved in N_2O production, but it may play a role in the amount of NO released by nitrifier denitrification. It was also confirmed that N_2O production by *N. europaea* follows a Michaelis-Menten model, which is a strong indicator of its enzymatic origin. All strains were able to remove varying concentrations of NO_2^- and presumably reduce it to NO, or N_2O in the case of *N. europaea*.

ZUSAMMENFASSUNG

Distickstoffmonoxid (N_2O) ist ein Treibhausgas, das von einer Vielzahl von Mikroorganismen, einschließlich ammoniakoxidierender Bakterien (AOB), produziert wird. Der enzymatische Weg für die N_2O-Produktion in AOB umfasst die sequenzielle Reduktion von Nitrit (NO_2^-) zu N_2O durch zwei Enzyme: Nitritreduktase (NIR) und Stickstoffmonoxid-Reduktase (NOR). In AOB wurden zwei potenzielle NORs identifiziert. Die cNOR ist bekannterweise an der Stickstoffmonoxid (NO)-Reduktion beteiligt, die Rolle der sNOR ist jedoch noch unklar.

Das Hauptziel dieser Studie war es, AOB mit unterschiedlichen genetischen Repertorien zu untersuchen, um die Hauptquellen der N_2O-Produktion und die Rolle der sNOR zu klären. Drei AOB-Stämme die alle eine NIR (NirK) besitzen, aber mit unterschiedlicher NOR-Zusammensetzung wurden verwendet: *Nitrosomonas europaea* Nm50 (cNOR und sNOR), *Nitrosospira multiformis* Nl13 (keine NORs) und *Nitrosospira briensis* Nsp1 (sNOR). Mit einem Mikrorespirationssystem wurden gleichzeitig Sauerstoff (O2), NO und N_2O in einer geschlossenen Glaskammer gemessen. Dieser Aufbau ermöglichte eine Substratinjektion zu beliebigen Zeitpunkten und die Beobachtung aller drei Gase in Echtzeit.

Die Ergebnisse zeigten, dass die sNOR nicht an der N_2O-Produktion beteiligt zu sein scheint, aber eine Rolle bei der Menge an NO spielen könnte, die durch die Nitrifizierer-Denitrifikation freigesetzt wird. Es wurde auch bestätigt, dass die N_2O-Produktion durch *N. europaea* dem Michaelis-Menten-Modell folgt, was ein guter Indikator für ihren enzymatischen Ursprung ist. Alle Stämme waren in der Lage, unterschiedliche Nitritkonzentrationen zu entfernen und vermutlich zu NO oder im Fall von *N. europaea* zu N_2O zu reduzieren

ACKNOWLEDGEMENTS

I would like to thank the Centre for Microbiology and Environmental Systems Science (CeMESS) and specifically the Division of Microbial Ecology (DOME) for providing me with all the resources I needed throughout this master's thesis. Without any exception, this was the best work environment a student could have hoped for.

Within DOME I specifically want to thank the nitrification group led by Univ.-Prof. Dr. Holger Daims and Prof. Dr. Dr. h. c. Michael Wagner for hosting me. Dr. Holger Daims readily agreed to officially supervise this thesis and made all the bureaucratic hurdles a breeze to work through. I could always rely on scientific input and encouragement from all group members, which greatly contributed to my work. Some group members, who were involved in this project, I want to give an explicit thank you:

Dr. Craig Herbold performed the initial genomic analysis and without his work, this project would not have been possible.

Dr. Andrew Giguere was always able to provide constructive feedback when I struggled with understanding soil ecology and chemistry during my experiments.

Dr. Anna Mueller introduced me to the world of portable O_2 optode and sprouted the idea of the experimental setup we used here. Without her help and enthusiasm, we would not have been able to produce these results.

Many thanks go to Dr. Petra Pjevac for supporting me and my work in so many ways. Her seemingly endless wealth of knowledge and ideas were indispensable. She always had an open ear and offered her support to so many people while always providing major contributions across the CeMESS.

My biggest thank you goes to Dr. Christopher Sedlacek, who was my mentor in the laboratory, helped me with writing and shaped my early career. He was always open and encouraged my ideas while providing many of his own. I'll miss our recurrent meetings where we worked through confusing results and got excited about them only to disprove them a week later. I really hope you will supervise many more students in the future.

Finally, I want to thank my friends and family for their continuous and genuine support. Specifically, my parents and grandparents. Without you, this would not have been possible.

INTRODUCTION

The human population along with the production of anthropogenic reactive nitrogen have spiked since the invention of the Haber-Bosch process in 1913 (Erisman and Larsen, 2013). Before its discovery, it was becoming clear that conventional methods of supplying reactive nitrogen would not meet the growing global food demands. The Haber-Bosch process allows the production of ammonia (NH_3) from unreactive atmospheric dinitrogen gas (N_2) on an industrial scale. Today it is abundantly available and applied to agricultural fields worldwide. Currently, the Haber-Bosch process is considered essential for modern agriculture and for feeding the world.

Agricultural fertilization with industrially fixed nitrogen is responsible for producing the crops that feed around half of the world's population today (Smil, 2001; Erisman *et al.*, 2008). However, this ability to increase the global agricultural output does not come without disturbing natural biogeochemical cycles and creating new environmental problems. According to the nine Planetary Boundaries defined by Rockström et al. (Rockström *et al.*, 2009) we have far surpassed the amount of industrial and natural biological nitrogen fixation our planet can sustain. Even with more recent models, which expanded the theoretical nitrogen boundary, we are still exceeding the limit of safe reactive nitrogen species in the Earth's biosphere (De Vries *et al.*, 2013; Steffen *et al.*, 2015; Richardson *et al.*, 2023). This excess reactive nitrogen has a negative and potentially irreversible effect on global biodiversity, climate, ecosystem resilience, and human health (Erisman *et al.*, 2011, 2013). These occur through two major losses of fixed nitrogen. First, with overfertilization, the leaching or runoff of reactive nitrogen from the soil into ground- and surface water can occur, reaching aquatic environments like rivers, lakes, or the ocean. There it can lead to eutrophic conditions, acidification, algal blooms, and anoxic zones. All of these environmental consequences contribute to the negative global effects mentioned above (Bobbink *et al.*, 2010; Payne *et al.*, 2013).

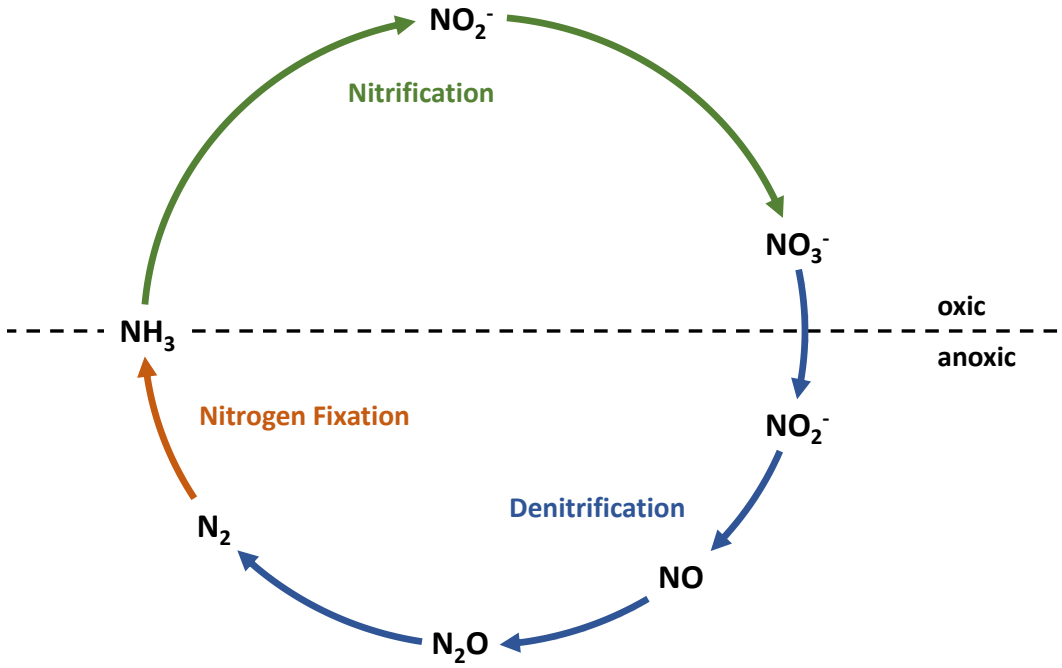

Figure 1: A simplified schematic of the biological nitrogen cycle. The three major processes of nitrogen fixation (orange), nitrification (green), and denitrification (blue) are highlighted. The cycle is separated by a dashed line, indicating the reactions that occur predominantly in oxic or anoxic environments.

Secondly, there is a major loss of fixed nitrogen to the atmosphere, where nitric oxide (NO) and nitrous oxide (N_2O) contribute to ozone layer depletion and global warming, respectively. N_2O is a stratospheric ozone-depleting greenhouse gas with an estimated lifetime of 116 ± 9 years (Prather *et al.*, 2015). Together with its potency and ever-increasing atmospheric concentration, it is deemed the third most important anthropogenic greenhouse gas behind carbon dioxide (CO_2) and methane (CH_4) (United Nations Environment Programme, 2013). Between 1750 and 2018 atmospheric N_2O concentrations have increased by more than 20%, with the fastest growth occurring in the past five decades (Hall, Dutton and Elkins, 2007; Prinn *et al.*, 2018; Tian *et al.*, 2020). The main contributing factors to the increased N_2O emissions have been identified as increased soil nitrification and partial denitrification linked to the overfertilization of agricultural soils (Smith, 1997; Griffis *et al.*, 2017; Pärn *et al.*, 2018; Tian *et al.*, 2019, 2020). Nitrification is the microbially mediated process during which NH_3 is oxidized to nitrate (NO_3^-) via nitrite (NO_2^-, Figure 1). This two-step reaction occurs in aerobic or microoxic environments and is carried out by a select group of microorganisms called nitrifying microorganisms.

Nitrifying microorganisms

The first isolated nitrifying microorganisms were ammonia-oxidizing bacteria (AOB) and nitrite-oxidizing bacteria (NOB) (Winogradsky, 1890), with AOB catalyzing the first and NOB

catalyzing the second step of nitrification. Phylogenetically the chemolithoautotrophic AOB, characterized by the prefix Nitroso-, and NOB, characterized by the pre-fix Nitro-, are not closely related (Teske *et al.*, 1996; Purkhold *et al.*, 2000). Nitrifiers can be found in a vast array of diverse environments including fresh and marine water, soil and wastewater treatment plants (WWTPs) (Klotz *et al.*, 2006; Norton *et al.*, 2008; Jia and Conrad, 2009; Ke, Lu and Conrad, 2015). Their combined ecophysiology gives them additional relevance in the biotechnological and agricultural sectors where ammonia oxidizers and nitrite oxidizers are either needed for the removal of NH_3 from wastewater (Yin, Bi and Xu, 2018) or responsible for fertilizer loss in agricultural soils (Zhou *et al.*, 2020). For over 100 years, these two types of microorganisms were considered to be the only microbial players responsible for microbial nitrification, regardless of environment or conditions.

Investigations into the ammonia monooxygenase (AMO) genes (*amoABC*), which encode the enzyme that facilitates the first step in bacterial nitrification (the oxidation of NH_3 to hydroxylamine), led to the discovery of the first *amoA* homolog belonging to an Archaeon. A subsequent screening in the environment for this homolog revealed a wide distribution of ammonia-oxidizing archaea (AOA) in terrestrial and aquatic ecosystems (Venter *et al.*, 2004; Francis *et al.*, 2005; Treusch *et al.*, 2005). Surprisingly, soon after their discovery, it was observed that AOA were more abundant than AOB in most environments (Venter *et al.*, 2004; Könneke *et al.*, 2005; Schleper, Jurgens and Jonuscheit, 2005; Treusch *et al.*, 2005). Like AOB, AOA complete only the first half of nitrification, the oxidation of NH_3 to NO_2^-.

More recently complete ammonia oxidation (comammox) by bacteria belonging to the genus *Nitrospira* was discovered and a representative was isolated into pure culture (Daims *et al.*, 2015; van Kessel *et al.*, 2015; Kits *et al.*, 2017). These organisms can perform full nitrification, both NH_3 and NO_2^- oxidation. The environmental distribution of comammox-like *amoABC* and hydroxylamine dehydrogenase (HAO) genes (*haoAB*) in published metagenomic datasets suggests that comammox bacteria are widespread in soil and freshwater ecosystems, WWTPs, and drinking water treatment systems (Daims *et al.*, 2015; van Kessel *et al.*, 2015; Palomo *et al.*, 2016; Pinto *et al.*, 2016). Interestingly, comammox bacteria have even been found to be the dominant ammonia oxidizer in a full-scale WWTP (Daims *et al.*, 2015). Due to comammox bacteria being the most recently discovered nitrifier, there are still a lot of unknowns and open questions (e.g. their contribution to agricultural N_2O formation, or how they compete against other nitrifying microorganisms). Physiological growth parameters and their abundance across different ecosystems will continue to be assessed in order to better define their ecological niche within nitrifying communities.

While AOB, AOA, and comammox are all ammonia oxidizers, they are also all aerobic microorganisms that require oxygen. In contrast, some bacterial nitrifiers are also capable of anaerobic ammonium oxidation (anammox) (van de Graaf *et al.*, 1995). Anammox bacteria differ from their aerobic counterparts as NH_3 is oxidized and NO_2^- is simultaneously reduced forming N_2 as the main end product of the anammox process (Kartal *et al.*, 2007). Anammox bacteria contain cytoplasmic anammoxosomes, which are membrane-bound compartments that make up 30–60% of the cell volume. Anammoxosomes harbor an unusual enzyme complex that is able to facilitate the production of hydrazine (N_2H_4) during the anammox process (Jetten *et al.*, 2001). The metabolic activity of these bacteria is strongly inhibited by oxygen, making them a key nitrifier in environments like the oceanic O_2 minimum zones (van de Graaf *et al.*, 1995). Recently, anammox bacteria have received a lot of attention for their application in wastewater treatment. When combined, partial conventional nitrifiers and anammox bacteria can efficiently remove nitrogen from high-strength organic wastewater. However, very long lag-phases are required in these plants and this application in wastewater treatment is therefore still a niche solution to global wastewater treatment (Jetten, Horn and van Loosdrecht, 1997; Jetten *et al.*, 2001). Due to their O_2-sensitive metabolism, their habitat does not often overlap with aerobic ammonia oxidizers.

In contrast, AOA, AOB, and comammox frequently co-occur in aerobic environments as they all depend on free NH_3 and O_2 for growth. AOA are the most abundant ammonia oxidizers accounting for up to 30% of the microbial plankton in oligotrophic oceans and 1-3% of the total microbes in soils and sediments, thus often outnumbering AOB by orders of magnitude (Karner, DeLong and Karl, 2001; Leininger *et al.*, 2006; Mincer *et al.*, 2007; Agogué *et al.*, 2008; Prosser and Nicol, 2008; Herrmann, Saunders and Schramm, 2009; Beman, Sachdeva and Fuhrman, 2010; Zhang *et al.*, 2010). However, even with a much smaller population size, AOB are often the ammonia oxidizer population that responds strongest to nutrient inputs and is responsible for the bulk of the NH_3 oxidation activity in many environmentally important ecosystems such as fertilized agricultural soils (Di *et al.*, 2009; Song *et al.*, 2016).

The physiology of aerobic ammonia oxidizers

The process of nitrification

All three types of aerobic ammonia oxidizers oxidize NH_3 to hydroxylamine (NH_2OH) through a multi-subunit membrane-bound AMO enzyme complex. In all cases, this initial step of NH_3 oxidation at the AMO requires the input of two electrons from the ubiquinone

pool in order to catalyze the oxidation of NH_3 to NH_2OH (Arp and Stein, 2003). This is where the known similarities between the AOA and AOB/comammox central metabolism stop. In AOB/comammox, the NH_2OH was previously thought to be oxidized directly to NO_2^- via a periplasmic HAO (Hooper, 1978; Hooper, Maxwell and Terry, 1978; Hollocher, Tate and Nicholas, 1981). This would result in four electrons being transferred to the ubiquinone pool, a mechanism proposed to occur via two cytochromes, c554 and c_M552 (Hooper *et al.*, 2005). However, in AOB and presumed in comammox, the HAO has recently been shown to oxidize NH_2OH to NO and not directly to NO_2^- (Caranto and Lancaster, 2017; Figure 2). In this revised model, the NH_2OH oxidation at the HAO yields only three electrons. Therefore, a second currently unknown enzyme, a nitric oxide oxidase/oxidoreductase (NOO), is needed to facilitate the oxidation of NO to NO_2^-. This step would yield one additional electron, still resulting in a total of four electrons gained for the oxidation of NH_2OH to NO_2^-. Interestingly, all AOB, but not AOA or comammox encode multiple copies of the AMO and HAO subunits. It was previously suggested that both AMO and HAO genes are isofunctional and knockouts of either one did not produce a significant phenotype (Hommes, Sayavedra-Soto and Arp, 2002). In AOA, no known HAO homolog has been identified, but there is evidence that NO plays a central role in the NH_3 oxidation pathway of AOA (Shen *et al.*, 2013; Martens-Habbena *et al.*, 2015). There are multiple genes encoding putative copper-containing nitrite reductases (Cu-NIR), which have been proposed to facilitate the reduction of NO_2^- to NO in AOA or the reverse reaction of oxidizing NO to NO_2^- (Hallam *et al.*, 2006; Walker *et al.*, 2010; Blainey *et al.*, 2011; Kim *et al.*, 2011; Spang *et al.*, 2012; Kozlowski *et al.*, 2016). So, although NO_2^- is the stoichiometric end product of NH_3 oxidation by AOA, the exact intermediates and enzymes involved in the central metabolism of AOA are still elusive.

As the HAO in AOB and comammox cannot oxidize NH_2OH directly to NO_2^-, a NOO would be beneficial to further facilitate the oxidation of NO to NO_2^- and gain an additional electron in these microorganisms. To date, the red copper protein nitrosocyanin (*ncyA*), and a reverse nitrite reductase (*nirK*) have been identified as potential NOO enzymes (Lancaster *et al.*, 2018). Nitrosocyanin and *nirK* are present in almost all AOB, while comammox bacteria only harbor the *nirK* and both genes expression often coincides with the other enzymes in the nitrification pathway (Bollmann *et al.*, 2013; Zorz *et al.*, 2018). Because nitrosocyanin is absent from comammox and not present in all AOB it cannot be the sole NOO in all ammonia oxidizers (Bollmann *et al.*, 2013; Daims *et al.*, 2015; van Kessel *et al.*, 2015; Kits *et al.*, 2019). However, their exact function in AOB/comammox (even aside from being a potential NOO) is still very unclear. Even though this enzymatic step is still missing

in AOB/comammox, it does not affect the end result of the NH_3 oxidation pathway: the production of nitrite.

The process of denitrification

Due to their sheer abundance in the environment, AOA likely contribute to global N_2O emissions through biotic and abiotic pathways. However, the enzymatic production of N_2O by AOA has so far only been demonstrated at low pH (Jung *et al.*, 2019) or during NO disproportionation under anoxic conditions (Kraft *et al.*, 2022). In both cases, the enzyme(s) responsible are currently under investigation. Similarly, AOB also produce N_2O through abiotic processes, and at atmospheric O_2 concentrations, the dominant N_2O producing pathway is the abiotic oxidation of NH_2OH (Hooper, 1968; Hooper and Terry, 1977; Hooper, Terry and Maxwell, 1977; Anderson *et al.*, 1993; Caranto and Lancaster, 2017; Mellbye *et al.*, 2018). Comammox, as the most recently discovered ammonia oxidizer, are severely understudied when it comes to their denitrification capabilities. Still, they have been shown to produce NO as an intermediate of NH_3 oxidation, which is abiotically denitrified to N_2O under oxic conditions (Kits *et al.*, 2017). However, this results in a generally low N_2O yield when compared to AOA and AOB (Liu *et al.*, 2017; Kits *et al.*, 2019; Han *et al.*, 2021). Unlike in the AOA and comammox, AOB also produce N_2O through an enzymatic process termed nitrifier denitrification (Figure 2). Nitrifier denitrification by AOB is a well-studied topic (Stein, 2011; Kozlowski, Price and Stein, 2014; Kozlowski, Kits and Stein, 2016a) and is known to occur across many different species (Jones *et al.*, 2015; Zhu-Barker *et al.*, 2015). Taken together, this leaves AOB as the main driver of enzymatic nitrifier denitrification in the environment (Kozlowski *et al.*, 2016), as many AOB encode the canonical genes necessary for the partial denitrification of NO_2^- to NO or N_2O (Stein, 2019).

Under anoxic or O_2-limited conditions, NO_2^- and NO can serve as alternative electron sinks in the enzymatic reduction of NO_2^- via NO to N_2O (Schmidt, van Spanning and Jetten, 2004; Cantera and Stein, 2007). The first step of nitrifier denitrification is the reduction of NO_2^-. In AOB, a copper-containing nitrite reductase (NirK) converts NO_2^- to NO (Schmidt, van Spanning and Jetten, 2004; Cantera and Stein, 2007; Kozlowski, Price and Stein, 2014). Previous screenings by low-stringency Southern blotting and PCR to identify DNA sequences with similarity to nirK revealed no hybridization signals from genomic DNA of *Nitrosococcus mobilis* Nc2, *Nitrosomonas cryotolerans* Nm55, or *Nitrosomonas communis* Nm2 (Cantera and Stein, 2007). Later, genome sequencing confirmed these observations in *Nitrosomonas communis* Nm2 (Kozlowski, Kits and Stein, 2016b). In addition, nirK-knockout mutants of *N. europaea* did not have completely diminished N_2O production (Beaumont *et al.*, 2002; Schmidt, van Spanning and Jetten, 2004), and produced more N_2O

than the wild-type (Cantera and Stein, 2007). These observations indicate the presence of additional unknown nitrite reductases, which contribute to nitrifier denitrification (Kozlowski, Price and Stein, 2014).

A nitric oxide reductase (NOR) reduces NO further to N_2O. To date, two membrane-bound cytochrome c oxidases (cNOR and sNOR), proposed to catalyze NO reduction to N_2O, have been identified in AOB (Cho *et al.*, 2006; Klotz and Stein, 2008; Kozlowski, Kits and Stein, 2016a). Out of these two, the cNOR has been proposed as the main contributor to NO reduction under anoxic conditions in AOB (Kozlowski, Price and Stein, 2014). A global transcriptome study of *N. europaea* without a *nirK* gene unveiled upregulation in two gene clusters (*coxAB* and *senC*/*sco1*) only found in AOB and a few sulfur oxidizers (Cho *et al.*, 2006). These gene clusters have previously been proposed as a NOR called sNOR encoded by *norSY* (Cantera and Stein, 2007). However, a sNOR enzyme has never been functionally characterized in any microorganism and its proposed role as a NOR has recently been questioned (Giuffrè *et al.*, 1999; Matsuda *et al.*, 2002; Füssel *et al.*, 2017; Murali *et al.*, 2021). While the norCBQD gene cluster is only slightly upregulated under O_2-limited growth, all genes of the sNOR (*norSY-senC*) were transcribed at significantly higher levels under these growth conditions (Sedlacek *et al.*, 2020). This suggests that under long-term O_2-limited conditions, sNOR may contribute to NO reduction during nitrifier denitrification, or it might function as a high-affinity terminal oxidase in *N. europaea*. The exact role of sNOR in AOB currently remains elusive.

Most studies investigating the N_2O-producing pathways in AOB have focused on a single strain of *N. europaea* (Beaumont *et al.*, 2002, 2004; Cantera and Stein, 2007; Kozlowski, Price and Stein, 2014; Yu and Chandran, 2010; Yu *et al.*, 2010). While this targeted approach has identified key differences between differences between AOB and AOA (Kozlowski *et al.*, 2016) and recently questioned the presence of NO as a free intermediate (Choi, Chaudhry and Martens-Habbena, 2023), few investigations into the differences in N_2O production profiles between species have been conducted. One notable exception is Kozlowski *et al.* 2016, where NO and N_2O production and consumption profiles of AOB during nitrification and denitrification were compared. Interestingly, regardless of their genetic repertoire for identifiable canonical denitrification genes, all the AOB produced measurable N_2O. This highlighted the previously unknown diversity of nitrifier denitrification resulting in the release of biotic and abiotic N_2O both in the presence and absence of O_2 by multiple AOB strains. However, NO is now recognized to be an intermediate during both nitrification and denitrification (Lancaster *et al.*, 2018). This makes it difficult to assign the production and consumption of NO and N_2O to solely the process of nitrification (with

additional abiotic processes producing N_2O from generated NO) or denitrification (NO and N_2O production from NO_2^-) (Figure 2) when AOB are oxidizing NH_3. In addition, there have been no studies with the simultaneous real-time detection of O_2, NO, and N_2O production and consumption profiles. This always resulted in either reporting two separate real-time production and consumption curve experiments (Kozlowski *et al.*, 2016; Kozlowski, Kits and Stein, 2016a) or endpoint isotope labeling experiments (Poth and Focht, 1985; Kozlowski, Price and Stein, 2014).

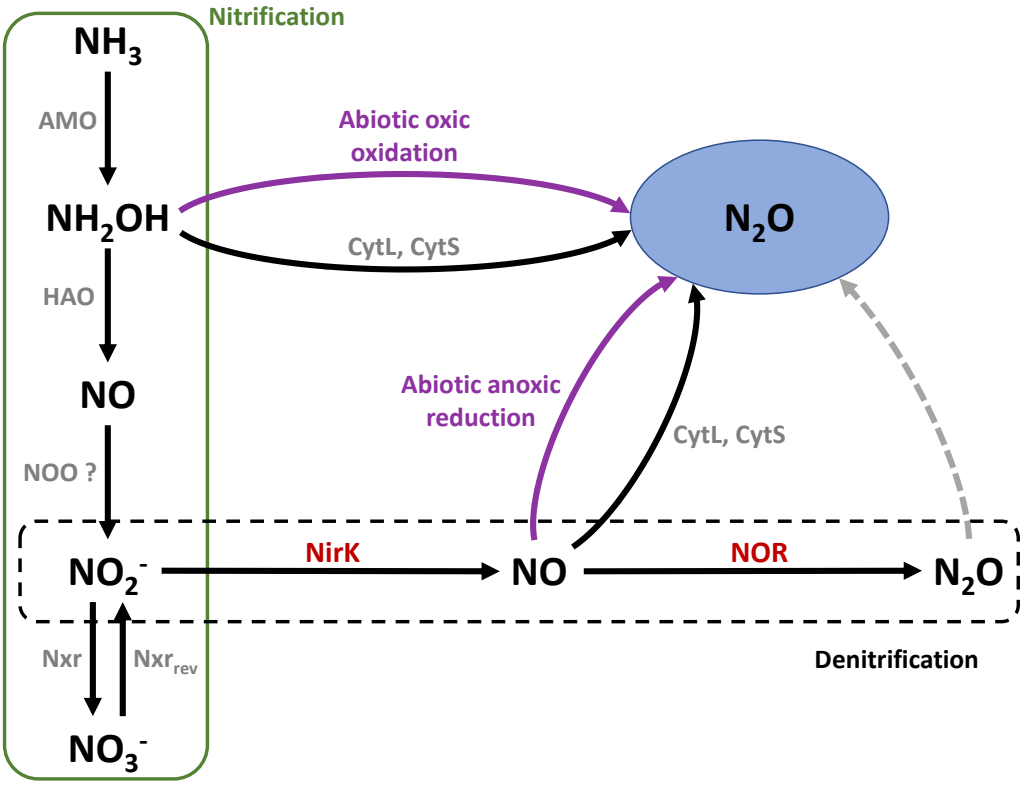

Figure 2: A simplified overview of the nitrification (green box) and partial denitrification pathway (dashed box) in AOB leading to N_2O production. Enzymatic process (black arrows), abiotic N_2O production (violet arrows), and the contribution of nitrifier denitrification to the total N_2O pool (dashed grey arrow) are indicated. AMO, ammonia monooxygenase; HAO, hydroxylamine dehydrogenase; NOO, nitric oxide oxidase/oxidoreductase; Nxr, nitrite oxidoreductase; NirK, nitrite reductase; NOR, heme-iron-containing nitric oxide reductase; c-type cytochrome P460 (CytL); c-type cytochrome c′-beta (CytS).

In this thesis, we aim to address both previously mentioned challenges: 1) we will separate the NO and N_2O production and consumption profiles that occur during nitrification and denitrification and 2) we will provide real-time simultaneous O_2, NO, N_2O production and consumption profiles during both nitrification and denitrification. Here, a microrespiration (MR) system was used with a modified glass chamber, allowing for the continuous measurement of NO and N_2O with two chemoelectrical sensors and O_2 with an internal O_2 optode. In addition, hydrazine (N_2H_4) was used as an alternative electron donor for nitrification in place of NH_3 or NH_2OH, as it is oxidized to N_2 by the HAO in AOB (Schalk *et*

al., 2000). Importantly, the oxidation of N_2H_4 in contrast to NH_3 or NH_2OH does not form NO or N_2O as side products or NO_2^- as an end product. Therefore, electrons gained through the oxidation of N_2H_4 are subsequently used by the terminal oxidase or nitrate reductase without creating any interfering nitrogen compounds. This allows for the introduction of NO_2^- after the bacterial cultures have reached anoxia, effectively separating the nitrification and denitrification process and their products.

To further improve our understanding of N_2O production in AOB through denitrification, we investigated three AOB strains with varying NOR genetic repertoire. The two main goals of this thesis were to 1) compare the NO and N_2O production profiles of these three AOB and 2) define the role of sNOR, or lack thereof, in anoxic N_2O production from NO. This work begins to clarify the role of sNOR in the physiology and metabolism of AOB and other microorganisms. Our results indicate that cNOR deficient AOB are unable to anoxically, enzymatically reduce NO to N_2O, regardless of the presence of sNOR. AOB lacking cNOR were able to reduce varying amounts of NO_2^- to NO without producing measurable N_2O.

METHODS

AOB strains and cultivation

Nitrosomonas europaea Nm50, *Nitrosospira briensis* Nsp1, and *Nitrosospira multiformis* Nl13 all have previously closed genomes and were all cultivated under the same conditions. AOB were cultivated in 2 L Schott bottles (1.3 L working volume), at 28°C, in the dark, without shaking, in a HEPES-buffered salt medium (Table 1). Cultures were checked weekly and 1-3 mM of sterile NH_4Cl was added before substrate depletion. Additionally, during culture refeeding, the pH was adjusted with 1 M of sterile $NaHCO_3$ to 7.8 - 8.0, and 1 mL of culture was added to 5 mL LB medium as a heterotrophic contamination control. Contamination growth tests were incubated at 37°C for at least two weeks, and any detectable microbial growth was regarded as heterotrophic contamination. The LB medium contained 0.5 g tryptone, 0.25 g yeast extract, and 0.5 g NaCl in 500 mL MQ water.

Table 1: Composition of HEPES buffered salt medium. All components were combined, and the pH was adjusted with 1 M NaOH prior to autoclaving. The TES and SWS were each added as 1 mL/L of medium from a 1000x stock solution. Substrate (NH_4Cl) and dissolved inorganic carbon ($NaHCO_3$) were added as needed at varying concentrations from previously sterilized stock solutions.

	Contains		**pH**
HEPES buffered salt medium	NaCl	0.584 g/L	~ 7.8
	KCl	0.075 g/L	
	$CaCl_2$ x 2 H_2O	0.011 g/L	
	$MgSO_4$ x 7 H_2O	0.024 g/L	
	KH_2PO_4	0.0544 g/L	
	HEPES	1 or 5 g/L	
Supplementary components added			
Trace Element Solution (TES)	$MnSO_4$ × 1 H_2O	34.4 µg/L	-
	H_3BO_3	50.0 µg/L	
	$ZnCl_2$	70.0 µg/L	
	Na_2MoO_4 × 2 H_2O	72.6 µg/L	
	$CuCl_2$ × 2 H_2O	20.0 µg/L	
	$NiCl_2$ × 6 H_2O	24.0 µg/L	
	$CoCl_2$ × 6 H_2O	80.0 µg/L	
	$FeSO_4$ × 7 H_2O	1.00 mg/L	
Selenite-Tungstate (Wolframate) Solution (SWS)	Na_2SeO_3 × 5 H_2O	3.00 µg/L	-
	Na_2WO_4 × 2 H_2O	4.00 µg/L	
	NaOH	0.50 mg/L	

AOB biomass harvesting for microrespiration (MR) experiments

For single MR chamber experiments, ~1 L of *N. briensis* Nsp1, ~1 L *N. multiformis* NI13, or ~500 mL of *N. europaea* Nm50 culture were harvested. This initial culture volume was sterilely concentrated through an Avantor® 0.2 µm PES bottle top filter. The concentrated biomass was resuspended with 100 mL of substrate-free 1 g/L HEPES buffered salt medium. The resuspended biomass was transferred to Amicon® Ultra-15 Centrifugal Filter Units (14,000 kDa cut off) and centrifuged (3000 G, 20°C, 15 min). The filtered supernatant

was removed, and the biomass was washed with 1 g/L HEPES substrate-free medium (at least three rounds of washing were performed). The concentrated biomass was resuspended in a total volume of 15 mL (representing a ~30-70x cell concentration) with substrate-free medium. Samples for chemical (NO_2^- and NO_3^-) and molecular (protein, qPCR, and 16S rRNA gene sequencing) analysis were taken before the MR experiments and stored at -20°C for subsequent analysis.

Microrespiration system setup

NO and N_2O were measured using an MR system (Unisense, Aarhus, Denmark). All experiments were performed in a 10 mL glass chamber equipped with two glass lids and two glass covered stir bars. Both lids had a capillary inlet to allow the insertion of Clark-type (Clark *et al.*, 1953) NO-MR and N_2O-MR microsensors (Unisense, Aarhus, Denmark). One of the lids additionally contained a silicone-covered injection port. The sensor signals of the NO-MR and N_2O-MR sensors were collected with a UniAmp Multi Channel picoammeter (Unisense, Aarhus, Denmark) and recorded using the SensorTrace Rate software (Unisense, Aarhus, Denmark). Both sensors were polarized for at least 24 hours according to the manual before use.

O_2 consumption was measured with a Trace Range Oxygen Sensor Spot (PyroScience, Aachen, Germany), which was fixed onto the inside wall of the 10 mL glass chamber with SPGLUE silicone (PyroScience, Aachen, Germany). A basic spot adapter (PyroScience, Aachen, Germany) was mounted to the outside of the chamber to align the SPFIB-LNS optical fiber (PyroScience, Aachen, Germany) with the O_2 sensor spot. The optical fiber was connected to a multi-analyte meter FireSting®-PRO (PyroScience, Aachen, Germany) and the signal was recorded with the Pyro Workbench (PyroScience, Aachen, Germany).

Sensor calibration

The O_2 sensor was calibrated with a two-point calibration. An anoxic solution was prepared with the addition of 0.2 g sodium ascorbate (Carl Roth, Karlsruhe, Germany) in 10 mL of 0.1 M NaOH. This solution was immediately put into the 10 mL MR chamber, sealed with glass lids, and submerged into a 28°C water bath for the 0 µM O_2 calibration point. Fresh 1 g/L HEPES buffered salt medium was used for the fully oxic calibration point (245 µM O_2). In each case, the optode reading was allowed to stabilize over the course of a few minutes, and multiple readings were recorded and averaged for the calibration curve.

The N_2O sensor was also calibrated with a two-point calibration with the N_2O Sensor Calibration Kit (Unisense, Aarhus, Denmark) with an upper detection limit of 94.2 µM N_2O.

The calibration was performed in the 10 mL MR chamber submerged in a 28°C water bath. After rinsing the chamber, the N_2O-free calibration point was taken with fresh HEPES buffered salt medium. In each case, the sensor was allowed to stabilize over the course of a few minutes, and multiple readings were recorded and averaged for the calibration curve.

To calibrate the NO sensor, a solution with 0.33 g potassium iodide (Sigma-Aldrich, Wien, Austria) in 20 mL of 0.1 M sulfuric acid was put into the 10 mL MR chamber, sealed with glass lids, and submerged into a 28°C water bath. After the sensor was allowed to stabilize the 0 µM NO calibration point was taken. Injections (5 µL) of varying NO_2^- concentrations into the chamber were performed. Through the reducing solution, NO was produced in a stoichiometric manner. After each injection, a calibration point was taken after sensor stabilization and the calculated amount of total NO in the chamber was noted. This resulted in a linear four-point calibration curve with an upper detection limit of 524 nM NO.

MR denitrification experiments

Concentrated AOB cultures (~15 mL; described above) were incubated in a 28°C water bath to recover from the biomass concentration procedure for at least 1 hour before the start of MR experiments. Double MR chambers (10 mL) were overfilled with concentrated AOB cultures to create a headspace free environment, before adding the magnetic stir bar and inserting the chamber lids. Filled chambers were submerged into the 28°C water bath, the stirring was set to 350 rpm, the NO- and N_2O-MR sensors were inserted, and the O_2 optode readout cable was attached. The biomass was left to equilibrate for 30-120 min before substrate injections, depending on the stability of the sensor readings and the background respiration of the biomass.

Once stable background respiration was achieved and the NO- and N_2O-MR sensor readings were stable, a 10 µL or 500 µL syringe (Hamilton, Bonaduz, Switzerland) with a 0.60 x 80 mm needle was used for substrate injections. Hydrazine sulfate (40 µL of 250 mM) was injected resulting in a final concentration of 1 mM N_2H_4 in the chamber. After complete O_2 depletion and the sensors stabilized again, NO_2^- injections of varying final concentrations followed in either a single individual injection or multiple additive injection scheme.

During the single injection scheme, 10 µL of varying NO_2^- concentrations were injected. After each NO_2^- injection, the sensors were left to stabilize again (hours to days). After all three sensors were stable again, additional NO_2^- injections into the chamber were performed in the same manner. Multiple additive injections were performed to investigate

the whole cell kinetics of the denitrification pathway in *N. europaea* Nm50. Here 10 µL (injections below 5 mM total NO_2^-) or 20 µL (injections above 5 mM total NO_2^-) were performed with varying NO_2^- stock concentrations. Injections were performed in approximate 10 min intervals, to allow for a stable slope of N_2O production to be recorded after each injection. The NO_2^- injections were performed until there was no longer an increase in the N_2O production rate. Samples for chemical (NO_2^- and NO_3^-) and molecular (protein, qPCR, and 16S rRNA gene sequencing) analysis were collected after all MR experiments and stored at -20°C for analysis.

MR chemical controls

Chemical controls in the absence of microbial biomass with various concentrations of ammonium salts (NH_4Cl, NH_4NO_3, and $(NH_4)_2SO_4$), N_2H_4, and NO_2^- were performed in oxic and anoxic HEPES-buffered salt medium. Anoxic medium was created by injecting a sodium ascorbate (in NaOH) solution (1.2 mL; see above) into the MR chamber. All controls were performed in the 10 mL MR chamber with all three sensors set up as described above. The chamber was submerged into a 28°C water bath and set to stir at 350 rpm.

Whole cell denitrification kinetic modeling

The maximum production rate (V_{max}) of N_2O and the apparent substrate affinity ($K_{m(app)}$) of NO_2^- were calculated from multiple NO_2^- injections and the resulting N_2O production rates. Three N_2O production profile biological replicates for *N. europaea* Nm50 were acquired. For each biological replicate, the total protein concentration in the MR chamber was measured (see below). The N_2O production rates of each replicate were normalized to the total amount of protein present in each biological replicate. The whole cell denitrification pathway kinetics were fit with a Michaelis-Menten model using the normalized N_2O production rate data across various NO_2^- concentrations (Equation 1). Due to the high variation in the calculated V_{max} values between the replicates, each replicate was plotted individually.

$$v = \frac{V_{\max}\,[S]}{K_{\mathrm{m}} + [S]}$$

Equation 1: Michaelis-Menten equation used for denitrification kinetic modeling. v, reaction rate; V_{max}, maximum production rate at saturating substrate concentration; K_m, Michaelis-Menten constant describing substrate affinity; $[S]$, substrate concentration.

Whole cell protein quantification

Protein quantification for the denitrification kinetic modeling was done with a Pierce™ BCA Protein Assay Kit. After each MR experiment, a 1 mL sample from the MR chamber was

spun down (20817 g, 5 min, 20°C) and the cell pellet was frozen at -20°C. After thawing the pellet, 100 µL of B-PER reagent was added to lyse cells. The enhanced test-tube procedure of the Pierce™ BCA Protein Assay Kit was followed as per the manufacturer's instructions.

Nitrite and nitrate measurements

NO_2^- and NO_3^- were determined spectrophotometrically using a modified Griess assay. The quantification protocol was adapted from previous high-sensitivity methods (Miranda, Espey and Wink, 2001; García-Robledo, Corzo and Papaspyrou, 2014). Samples analyzed were taken directly after washing the biomass, from the chamber at the end of MR experiments, and from leftover biomass which was kept in the water bath but never entered the MR chamber. All samples were frozen at -20°C before analysis. Three reaction solutions were prepared: i) Vanadium(III)-chloride (VCl_3) solution with 500 mg VCl_3 in 50 mL 1 M HCl, ii) N-naphthyl ethylenediamine dihydrochloride (NEDD) with 100 mg NEDD in 100 mL MQ water and iii) sulfanilamide solution with 2.5 g sulfanilamide in 250 mL 3 M HCl. A standard curve between 0.098 µM - 50 µM NO_2^- and NO_3^- was prepared in HEPES buffered salt medium. On a 96-well plate 270 µL sample/standard were mixed with 27 µL of a Sulfanilamide and NEED master mix (4:1). After incubation in the dark at room temperature (10 min), the absorbance was measured at 545 nm to determine NO_2^- concentrations. The VCl_3 solution (25 µL) was added, the plate was sealed with plastic foil, and incubated at 60°C for 30 min. The plate was cooled to room temperature and the absorbance was again measured at 545 nm to determine NO_x concentrations. NO_2^- concentrations were subtracted from the NO_x measurement to acquire the NO_3^- concentration of the samples.

RESULTS

AOB comparative genomics

Recently, whole genome sequencing of more than 80 genomes derived from cultured and isolated AOB was performed, resulting in a wealth of closed or high-quality draft AOB genomes (Herbold et al., 2023; in preparation). Here, this genomic library with known cultured representatives was viewed as a quasi-AOB knockout library and used to select the three AOB strains utilized in this study (*Nitrosomonas europaea* Nm50, *Nitrosospira briensis* Nsp1, and *Nitrosospira multiformis* Nl13). A comparison of the gene inventory of these three AOB revealed similarities in genes essential for nitrification but key differences in their denitrification genetic repertoire (Table 2).

All three AOB strains encode at least one full copy of the *amoCABED and haoAB-cycAB* gene cluster encoding the AMO and HAO complex subunits respectively (Table 2). As all

three AOB have previously been isolated as chemolithoautotrophs with the ability to grow aerobically with NH_3 as their sole energy source, this energy generation gene repertoire was expected. In addition, all three AOB strains encode a low-affinity cyt *c aa3* (A1 type) heme-copper-oxidase (HCO) but lack either a high-affinity cyt c *cbb3* (C type) HCO or a quinol-oxidizing *bo3*-type oxidase, which are encoded by some other AOB species/strains. The three selected AOB isolates harbor a diverse set of genes encoding for enzymes involved in nitrogen oxide metabolism and nitrogen oxide sensing (Table 1). However, the exact role or function of many of these is currently unknown. Despite differences, all three encoded the AOB-specific red copper protein nitrosocyanin, a redox-sensitive possible electron carrier (Arciero *et al.*, 2002; Sayavedra-Soto and Arp, 2014), and cytochrome c' beta (CytS) (Table 2).

The three AOB used in this study were specifically selected for their distinct set of genes related to the partial denitrification of NO_2^- to N_2O (Table 2). All three encode for a periplasmic copper-containing nitrite reductase enzyme (*nirK*), that carries out the one electron reduction of NO_2^- to NO. However, each AOB harbors a different set of NOR genes/proteins responsible for the subsequent step of denitrification, the one electron reduction of NO to N_2O. *N. europaea* Nm50 has one copy of the canonical heme-iron-containing nitric oxide reductase cNOR encoded by the *norCBQD* gene cluster and one copy of the putative heme-copper-containing nitric oxide reductase sNOR gene cluster (*norSY-senC-orf1*). In contrast, *N. briensis* Nsp1 does not encode the canonical cNOR but has one copy of the sNOR genes and *N. multiformis* NI13 lacks known NOR genes (Table 2). To date, the denitrification capabilities of *N. briensis* species containing only the sNOR gene cluster have not been explored.

It has been hypothesized that a lack of NOR genes is a consequence of growth in substrate-limited environments where there is no accumulation of nitrogen oxides and therefore little nitrosative stress (Hooper and Terry, 1979; Kozlowski, Kits and Stein, 2016a). *N. europaea* Nm50 and *N. multiformis* NI13 contain the cytochromes CytL (P460) and CytS (c'beta), while N. briensis Nsp1 lacks cytochrome CytL (P460). Both cytochromes have been proposed to alleviate nitrosative stress by oxidizing NH_2OH and NO to N_2O thereby expressing NOR activity (Elmore *et al.*, 2007; Klotz and Stein, 2008; Caranto, Vilbert and Lancaster, 2016). In addition, the NO-responsive transcriptional regulators *nsrR* and *nnrS* were both found in *N. europaea* Nm50. *N. briensis* Nsp1 only encodes the *nsrR* gene, and in *N. multiformis* NI13 both transcriptional regulators were not found (Table 2).

Table 2: Presence (+) or absence (-) of enzymes involved in nitrification or denitrification based on publicly accessible genomes. In addition, the presence or absence of terminal oxidases is shown. (+, ++ or +++) represents 1, 2, or 3 operons found in the genome respectively. AMO, ammonia monooxygenase; HAO, hydroxylamine dehydrogenase; NirK, nitrite reductase; cNOR, canonical heme-iron-containing nitric oxide reductase; sNOR, putative heme-copper-containing nitric oxide reductase; CytL, c-type cytochrome P460; CytS, c-type cytochrome c′-beta; NsrR and NnrS, NO-responsive transcriptional regulator; aa3, low-affinity heme-copper-containing terminal oxidase (A1 type); cbb3, high-affinity heme-copper-containing terminal oxidase (C type); bo3, quinol-oxidizing terminal oxidase.

			Nitrosospira		***Nitrosomonas***
			briensis	***multiformis***	***europaea***
			Nsp1	Nl13	Nm50
Nitrification	AMO	*amoCABED*	+++	++	++
	HAO	*haoAB-cycAB*	+++	+++	+++
Denitrification	**NirK**	***nirK***	**+**	**++**	**+**
	cNOR	***norCBQD***	**-**	**-**	**+**
	sNOR	***norSY-senC-orf1***	**+**	**-**	**+**
	Nitrosocyanin	*ncyA*	+	+	+
	CytL (P460)	*cytL*	-	+	+
	CytS (c'beta)	*cytS*	+	+	+
	NsrR	*nsrR*	-	-	+
	NnrS	*nnrS*	+++	-	+++
Terminal oxidases	aa3	*aa3*	+++	+	+
	cbb3	*cbb3-senC-orf1*	-	-	-
	bo3	*bo3*	-	-	-

Abiotic NO and N_2O production

Several abiotic chemical controls were performed with the substrates used during the microrespiration (MR) experiments. All the controls were done in either oxic or anoxic HEPES-buffered salt medium. Chemical controls with several ammonium salts were performed and a ~ 10 nM signal per 1 mM NH_4^+ injected was recorded with the NO sensor. This signal was consistent when injecting NH_4Cl, NH_4NO_3, and $(NH_4)_2SO_4$ in both oxic and anoxic chamber environments (Figure 3 A-D). Further experiments revealed that a combination of NH_4^+ and HEPES was responsible for the interference of the NO sensor. The concentration of HEPES and NH_4^+ in the chamber was directly proportional to the interference signal recorded by the NO sensor.

In addition, the interaction between N_2H_4 and NO_2^- was investigated. Here, in both oxic and anoxic environments, the N_2O sensor recorded a stable 1-2 µM signal when 1 mM N_2H_4 was injected into a chamber with at least 150 µM NO_2^- present. However, an injection of 150 µM NO_2^- into a chamber with 1 mM N_2H_4 did not elicit the same response under anoxic conditions (Figure 3 E).

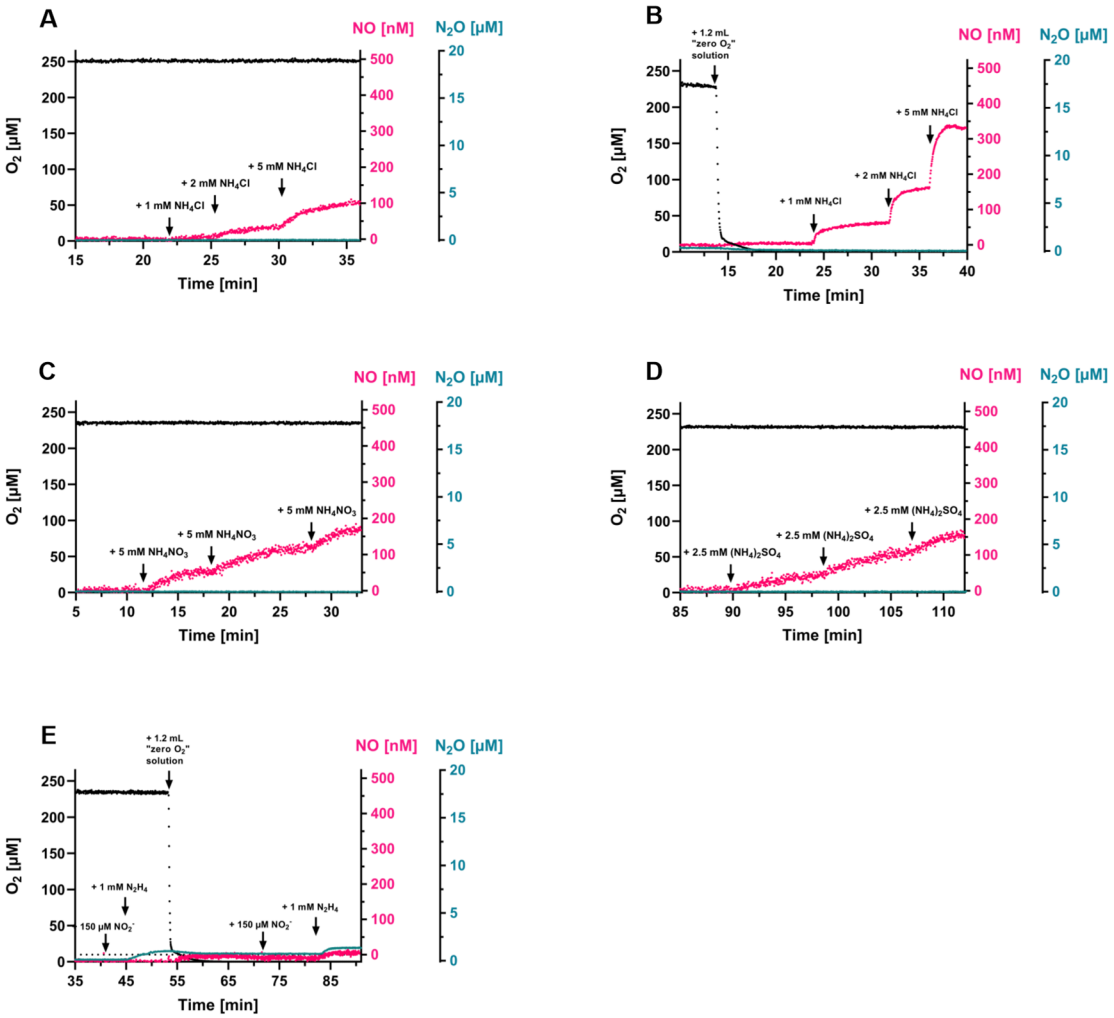

Figure 3: Selection of chemical controls done in HEPES buffered salt medium. The "zero O_2" solution consists of 0.2 g sodium ascorbate in 10 mL 0.1 M NaOH. In each panel, injections (5 µL) of either NH_4Cl, NH_4NO_3, $(NH_4)_2SO_4$ or N_2H_4 are indicated with arrows.

NO and N_2O dynamics with ammonia as a substrate

All three AOB strains were investigated for their denitrification capabilities with their natural substrate (NH_3) in MR experiments. Therefore, NH_4Cl was added to each MR chamber to a final concentration of 5 mM and the production and consumption curves of NO and N_2O were monitored as O_2 was depleted (Figure 4). Each AOB immediately produced NO after the initial NH_4Cl injection, however, all three produced distinct NO profiles. *N. europaea* Nm50 produced more than 500 nM of NO almost instantaneously, an amount which decreased when O_2 approached zero, but increased again during the anoxic phase. In contrast, *N. briensis* Nsp1 produced ~100 nM NO which remained stable until the MR chamber reached anoxia. At anoxia, the NO concentration rose quickly to above the detection limit of the NO sensor (500 nM). *N. multiformis* NI13 also produced about ~100 nM NO, which remained stable for about 30 minutes, before exponentially increasing to above 500 nM as the MR chamber reached anoxia (Figure 4). It is important to note that

NO detection during oxic conditions likely indicates NO formation as an intermediate of nitrification, from NH_2OH either enzymatically (CytL and CytS) or abiotically (explained above).

Even with different NO profiles, the oxic phase N_2O profiles of *N. briensis* Nsp1 and *N. multiformis* NI13 were very similar (Figure 4 B, C). Here, no N_2O signal was detectable until the MR chamber reached anoxia, at which point N_2O concentrations increased in a non-linear fashion (Figure 4). Interestingly, the N_2O concentration profile of *N. europaea* Nm50 showed N_2O continuously increasing while O_2 was still present in the MR chamber, and then remaining largely stable once anoxia was reached (Figure 4). Notably, high concentrations of NO lead to a cross-interference signal in the N_2O sensor, and therefore the N_2O concentrations observed during the very high NO peaks in all three AOB cannot be considered a result of biotic denitrification with certainty. Therefore it is difficult to tell, which N_2O sensor signal is real and where the N_2O is coming from.

Due to the problems caused by very reactive and cross-reactive intermediates, an alternative electron donor was used to separate the nitrification and denitrification profiles of the AOB. For this purpose, we used N_2H_4 as an electron donor and the precise addition of NO_2^- as the substrate for denitrification. All experiments moving forward were performed in this manner to allow better control over the amount of NO produced, to limit the cross-interference signal, and be able to fully resolve denitrification starting from NO_2^-.

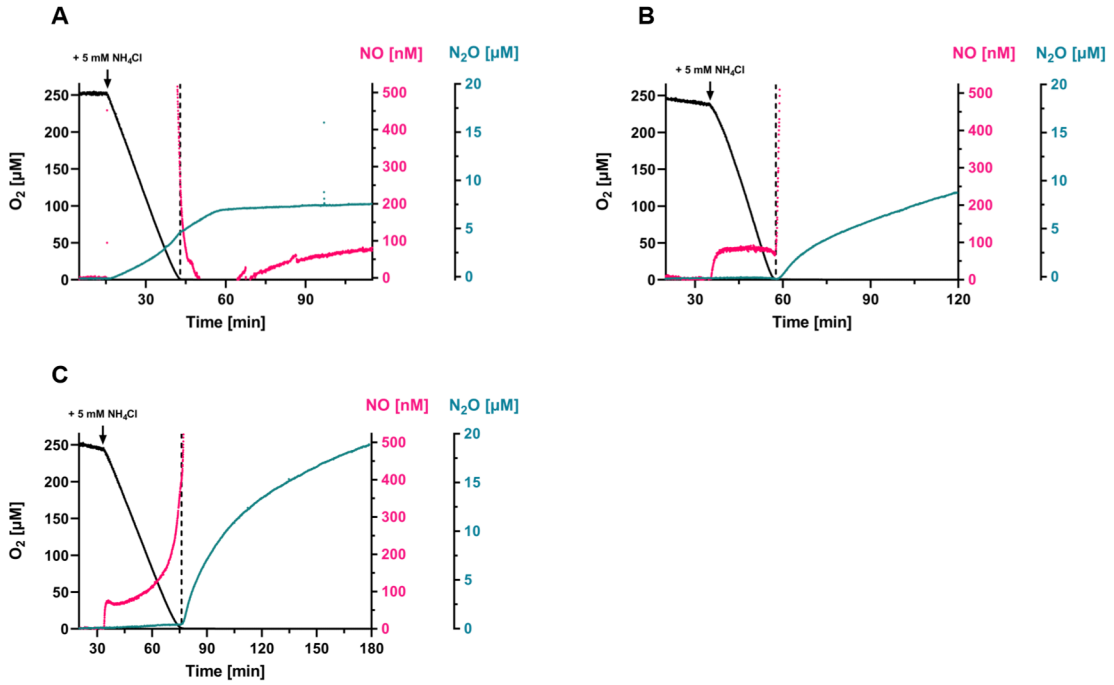

Figure 4: Measurements of O_2 consumption and NO/N_2O production and consumption during the oxidation of 5 mM NH_4Cl. *N. europaea* Nm50 **(A)**, *N. briensis* Nsp1 **(B)**, *N. multiformis* NI13 **(C)**. The dashed line indicates when each chamber dropped below 1 µM O_2.

NO and N_2O dynamics with N_2H_4 as a substrate

As an alternative to NH_3, the viability of N_2H_4 to be used as the sole electron donor for O_2 reduction without NO or N_2O generation was investigated. It is important to note that N_2H_4 was always injected in excess (1 mM final chamber concentration) to provide a constant source of electrons throughout the experiments. With N_2H_4 as the sole substrate, all three AOB were able to remove all the O_2 from a MR chamber. In addition, during O_2 depletion NO and N_2O remained below the limit of detection prior to chamber anoxia (Figure 5). This confirms that as an alternative substrate for the HAO, N_2H_4 donates electrons to the terminal oxidase(s) without producing reactive nitrogen species as intermediates. Therefore, N_2H_4 was used as the sole electron donor throughout the rest of the study.

Although NO or N_2O were undetectable during O_2 depletion, a burst of transitory NO was reproducibly observed at the onset of anoxia with *N. briensis* Nsp1 and *N. multiformis* NI13 strains (Figure 5 and Figure 6). However, NO and N_2O remained undetectable after anoxia was reached with *N. europaea* Nm50 (Figure 5 A). The maximum NO concentration reached during the NO anoxia bursts differed with each biological replicate. However, in general, the NO bursts were more pronounced with *N. multiformis* NI13 (>400 nM NO, Figure 5 C, Figure 6 I-L), than with *N. briensis* Nsp1 (<100 nM NO, Figure 5 B, Figure 6 E-H). In both strains, the NO disappeared entirely after a couple of hours. Although a small transitory N_2O peak was observed to overlap with the anoxia NO bursts for *N. multiformis* NI13, this is likely the

result of the known cross-sensitivity of the N_2O sensor to NO present in the MR chambers (see above).

The production of NO was not predicted as the biomass was washed free of detectable reactive nitrogen species (NH_4^+ and NO_2^-) and was not yet supplemented with external NO_2^-. Surprisingly, extracellular NO_2^- was detectable in control biomass samples from all three AOB, incubated at 28°C for the duration of the MR experiments (Table 3). This suggests that a certain amount of NO_2^- is retained intracellularly, or produced from intracellular ammonia/nitrogen storage, resulting in a low background amount of NO_2^- which is reduced to NO upon anoxia by *N. briensis* Nsp1 *and N. multiformis* NI13. Importantly, this transitory NO peak observed in *N. multiformis* NI13 and *N. briensis* Nsp1 react away, leaving zero nitrification intermediates in the MR chamber after several hours. Only after the NO stability returned to zero, were NO_2^- injections performed for denitrification experiments.

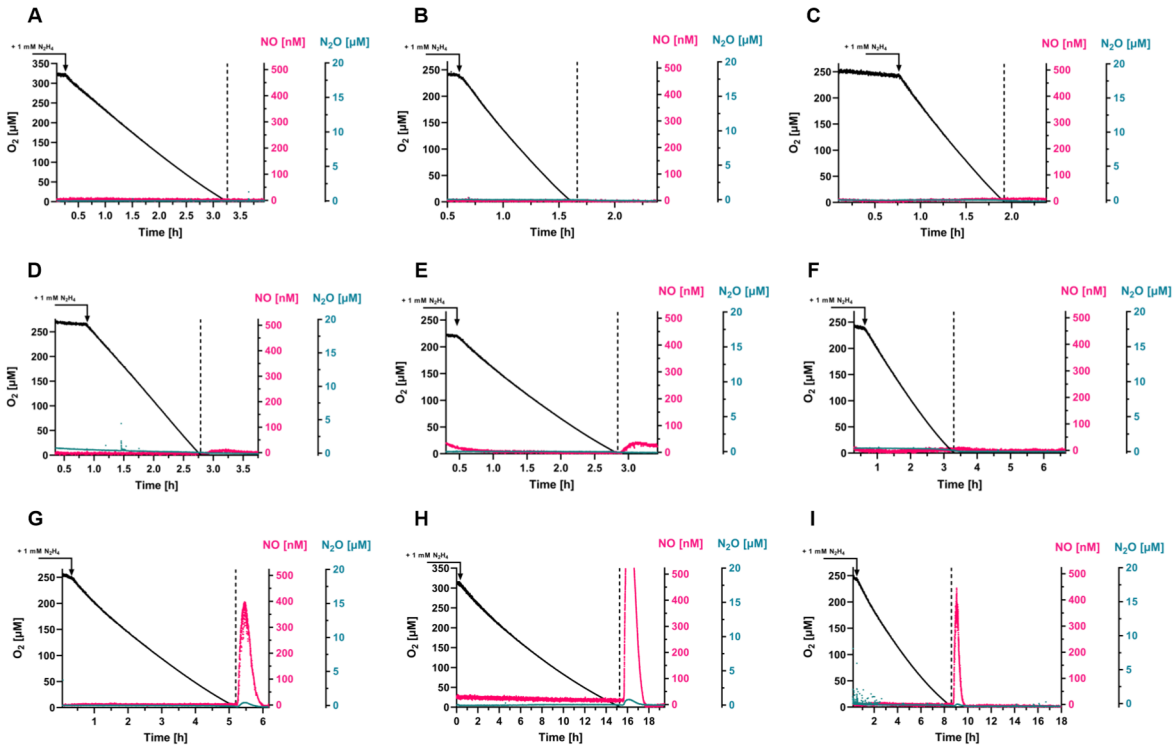

Figure 5: Measurements of O_2 consumption and NO/N_2O production after substrate (1 mM N_2H_4) injection. *N. europaea* Nm50 **(A-C)**, *N. briensis* Nsp1 **(D-F)**, *N. multiformis* NI13 **(G-I)**. The dashed line indicates when the chamber dropped below 1 µM O_2 in each chamber. The dashed line indicates when the chamber dropped below 1 µM O_2.

Table 3: Nitrite (NO_2^-) concentrations during the MR experiments. NO_2^- concentrations were measured from samples taken after washing the biomass, from samples, that were left to sit in substrate-free medium for the duration of an MR experiment to measure NO_2^- released by the biomass, and from samples taken at the end of a MR run directly from the chamber. NO_2^- released by the biomass is the amount of NO_2^- measured after letting the biomass sit for the duration of the MR experiment minus the NO_2^- measured after washing the biomass. NO_2^- left over from the injected amount, describes the NO_2^- measured after the experiment divided by the total amount of NO_2^- injected. (-) indicates samples, which could not be measured.

AOB strain	NO_2^- after washing biomass [µM]	NO_2^- released by biomass [µM]	NO_2^- left in chamber [µM]	NO_2^- left over from the injected amount	Figure
N. europaea Nm50	3.25	2.84	0	0 %	6 A
	2.53	15.62	4.53	18.10 %	6 B
	2.53	11.62	10.33	20.66 %	6 C
	2.84	1.41	0	0 %	6 D
N. briensis Nsp1	5.45	2.62	2.97	1.85 %	6 F
	-	-	0.88	1.47 %	6 G
	7.98	1.36	2.41	1.50 %	6 H
N. multiformis NI13	3.40	0.92	0.24	9.71 %	6 J
	2.92	0.57	0	0 %	6 K

NO and N_2O dynamics during denitrification

The denitrification capabilities of *N. europaea* Nm50, *N. briensis* Nsp1, and *N. multiformis* NI13, were determined with distinct single NO_2^- injections (0.5 - 100 µM) into anoxic MR chambers. Here, N_2H_4 was again used as the sole electron donor. Although multiple NO_2^- injections were performed in individual chambers for *N. briensis* Nsp1 and *N. multiformis* NI13, NO_2^- was only injected once NO concentrations in the MR chambers were stable and at or near zero (Figure 6). The NO and N_2O dynamics in all three AOB looked vastly different.

In the case of both *N. briensis* Nsp1 and *N. multiformis* NI13, bursts of NO production immediately followed each NO_2^- injection (Figure 6 E-L). In all cases, regardless of the NO_2^-

concentration introduced (0.5 - 100 µM), the NO concentration increased quickly, before peaking and subsequently returning to zero. The maximum amount of NO observed and the amount of time taken before the NO in the MR chamber returned to zero was dependent on the amount of NO_2^- injected and the AOB present. For example, *N. multiformis* NI13 produced NO beyond the upper calibration limit (524 nM) with 10µM NO_2^- (Figure 6 I). In *N. briensis* Nsp1 however the same NO_2^- concentration only produced ~70 nM NO (Figure 6 E). In all *N. briensis* Nsp1 and *N. multiformis* NI13 replicates (Figure 6 E-L) most of the NO_2^- was gone at the end of the experiment. Less than 3% of the injected NO_2^- was detectable at the end of MR experiments across all *N. briensis* Nsp1 replicates (maximum total amount of NO_2^- injected was 160 µM) and less than 0.25% across all *N. multiformis* NI13 replicates (maximum total amount of NO_2^- injected was 62.5 µM). Therefore, all the NO_2^- in the chamber was reduced, even in the cases where there was zero detectable NO or N_2O at the end of a MR experiment.

While N. briensis Nsp1 and *N. multiformis* NI13 were able to reduce all the provided NO_2^- to NO, stable N_2O concentrations were not detected in most biological replicates (see text above about transient N_2O sensor signals and NO and N_2O sensor cross talk). The exception was when *N. briensis* Nsp1 and *N. multiformis* NI13 were subjected to 100 µM or 50 µM NO_2^- injections respectively. Here, the NO generated greatly exceeded the upper detection limit of the NO sensor (524 nM) and remained above this limit for >6 hours in both cases. In these cases, stable N_2O concentrations remained for *N. briensis* Nsp1 (5.5 µM; >7 hours) and *N. multiformis* NI13 (17.2 µM; >1.5 hours) after NO depletion (Figure 6 H, L).

In stark contrast to *N. briensis* Nsp1 and *N. multiformis* NI13, *N. europaea* Nm50 immediately produced N_2O upon 10 - 100 µM NO_2^- injection without any detectable NO buildup (Figure 6 A-D). The two replicates where 10 µM and 100 µM NO_2^- where injected didn't have any NO_2^- left at the end of the MR run. In the experiments where 25 µM and 50 µM NO_2^- were injected 4.5 (18%) and 10.3 µM (21%) NO_2^- were still left at the end of the run. In addition, the N_2O produced by *N. europaea* Nm50 was stable and did not decrease over the course of several days (Figure 6 B, C).

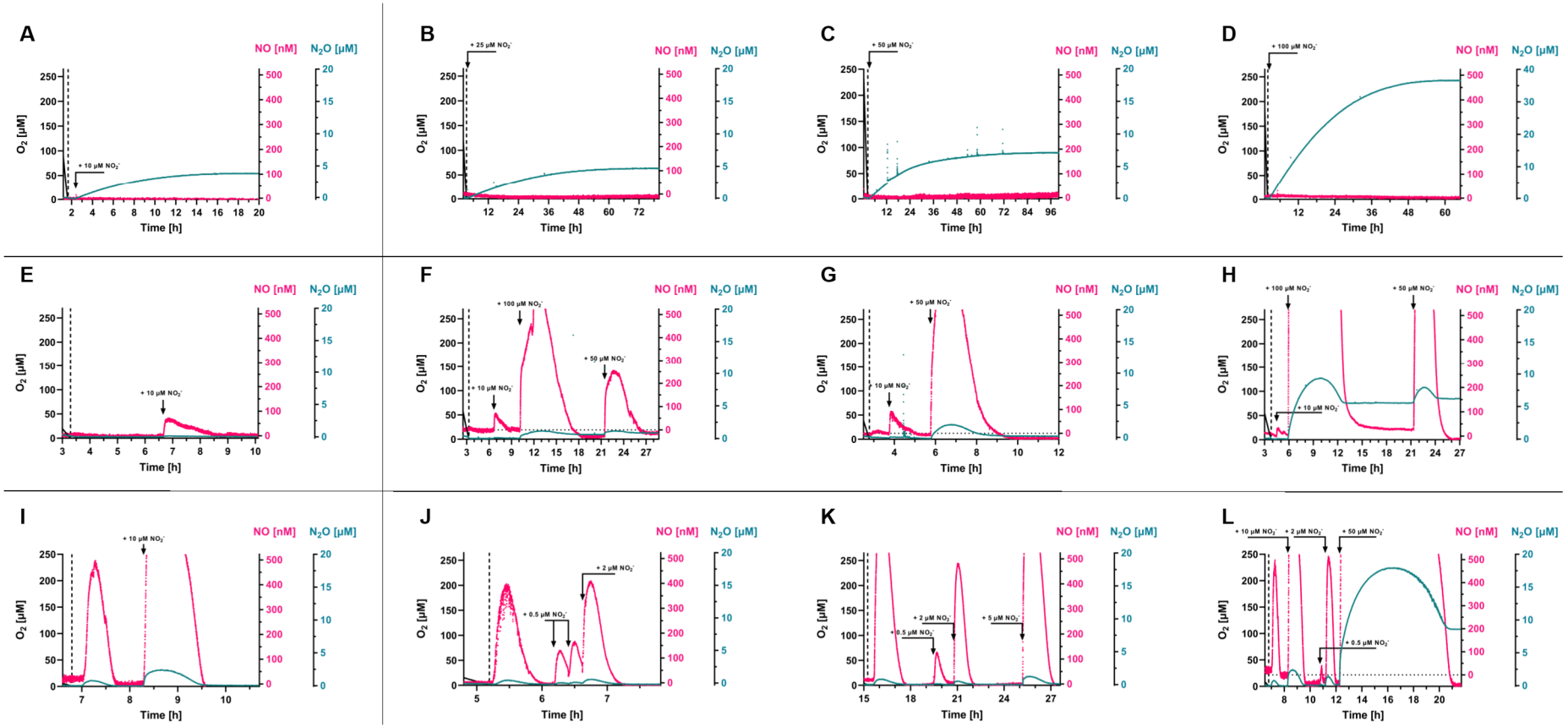

Figure 6: Measurements of O_2 and NO/N_2O production and consumption after injecting 1 mM N_2H_4 and subsequent NO_2^- injections. Only the anoxic part of the experiment is highlighted here (the vertical dashed line indicates where the chamber is at 1µM O_2). *N. europaea* Nm50 **(A-D)**, *N. briensis* Nsp1 **(E-H)**, *N. multiformis* Nl13 **(I-L)**. Panels **A**, **E** and **I** show only a 10 µM NO_2^- injection for easier comparison between strains. Panels **E** and **I** show the same data as **F** and **J** but with a shorter x-axis. A horizontal dotted line indicates the calibrated 0 µM for the NO sensor. NO_2^- concentrations at the end of each chamber were 0 µM **(A)**, 4.53 µM **(B)**, 10.33 µM **(C)**, 0 µM **(D)**, 2.97 µM **(F)**, 0.88 µM **(G)**, 2.41 µM **(H)**, 0.24 µM **(J)**, and 0 µM **(K)** (also see Table 3).

Whole cell denitrification kinetics of *N. europaea* Nm50

N. europaea Nm50 was the only AOB tested here capable of producing N_2O in response to supplemental NO_2^- in an anoxic environment independently of the NO_2^- concentration provided. Therefore, the whole cell partial denitrification pathway kinetics were determined for *N. europaea* Nm50. A multiple substrate injection method was used for the kinetic experiments, and they were conducted in the same MR chamber setup. Whole-cell kinetics of the *N. europaea* Nm50 denitrification pathway were modeled with a Michaelis-Menten based approach using the production rate of N_2O across a range of NO_2^- concentrations. For each biological replicate, the N_2O production rate was normalized to the total protein concentration in each MR chamber. All three biological replicates obtained are represented as individual panels (Figure 7). The protein normalized maximum production rate (V_{max}) of N_2O production ranged from 1.79 - 6.65 µM N_2O/h/mg protein with a standard deviation (SD) of ± 2.18 µM N_2O/h. The apparent substrate affinity ($K_{m(app)}$) for NO_2^- ranged from 1.28 - 1.84 mM NO_2^- with an SD of ± 0.23 mM NO_2^-.

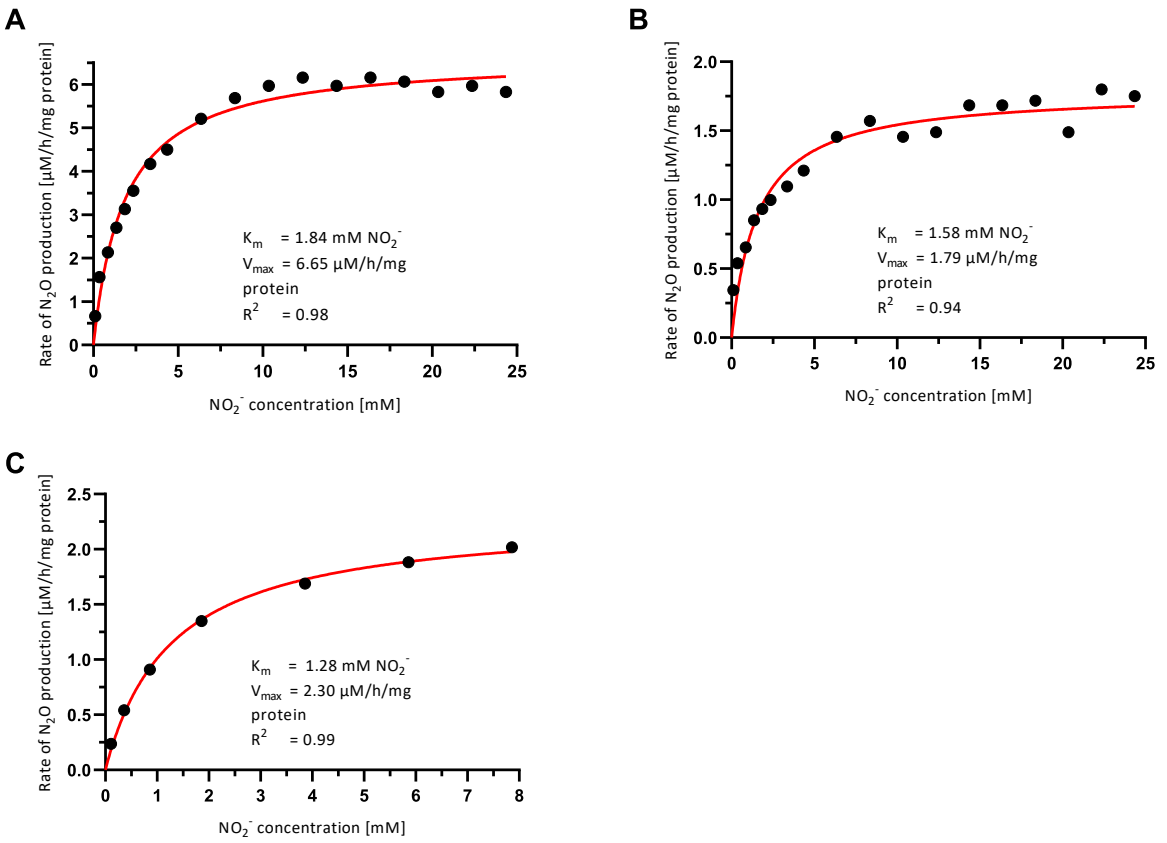

Figure 7: Denitrification kinetics of *N. europaea* Nm50. N_2O production rates were calculated from N_2O microsensor measurements after NO_2^- injections. The apparent substrate affinity ($K_{m(app)}$) for NO_2^- and maximum production rate (V_{max}) of N_2O were calculated by fitting the data to the Michaelis-Menten kinetic equation. The red line shows the best fit for the respective data. The three panels shown here are biological replicates. The standard deviation between them is ± 2.18 µM N_2O/h/mg protein for the V_{max} and ± 0.23 mM NO_2^- for the $K_{m(app)}$.

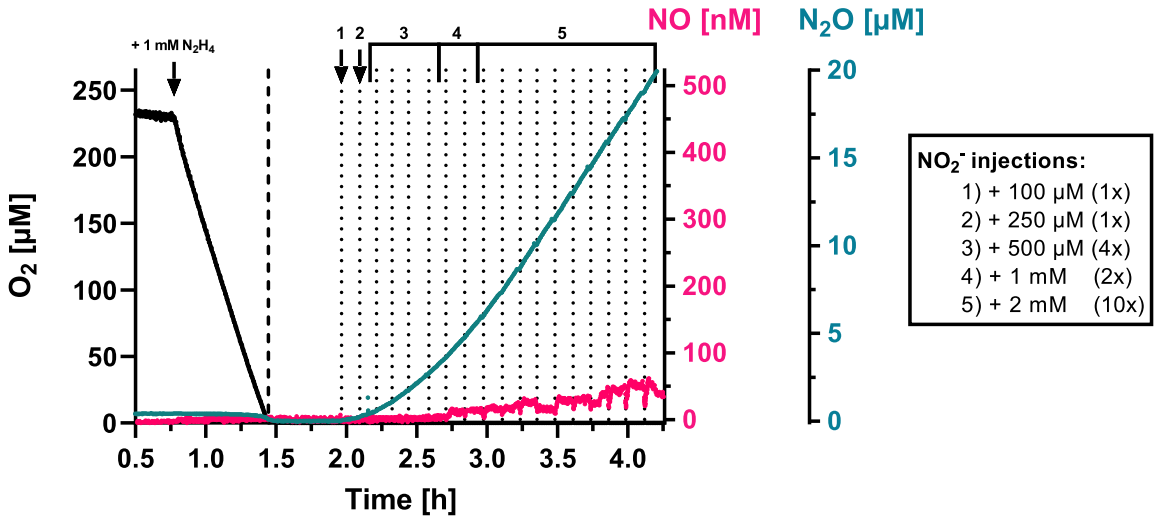

Figure 8: Example of multiple NO_2^- injections into a MR chamber with *N. europaea* Nm50 for denitrification kinetics measurements. NO_2^- injections are indicated by dashed lines while the amount of one injection can be seen by the number above and the figure legend to the right. At very high NO_2^- concentrations (>4 mM) NO becomes detectable for the first time and starts to build up slowly.

DISCUSSION

In this study, the goal was to compare NO and N_2O production and consumption profiles of AOB with differences in annotated genes related to denitrification. With the use of N_2H_4 as an electron donor and a setup that allowed for the simultaneous real-time observation of O_2, NO, and N_2O, the results presented here are more comprehensive than in previous studies. In addition, the results suffer less from the interference of reactive nitrogen species created when NH_3 or NH_2OH are used as electron donors. Therefore, some results from previous studies were confirmed here, but novel insights into nitrifier denitrification were also gained.

The use of N_2H_4 as an alternative substrate

The biggest difference to previous studies was the use of N_2H_4 as an electron donor in place of NH_3 or NH_2OH. The most prominent result of this can be seen during the oxic phase of all the MR data shown here. In all the experiments presented, the amount of N_2H_4 injected (1mM) provided enough energy for the AOB to reduce all of the O_2 present in the MR chambers through terminal oxidase turnover and also to fuel partial denitrification pathways. In addition, no strain produced any detectable NO or N_2O during oxic conditions when only N_2H_4 was present as an electron donor. Studies utilizing NH_3 or NH_2OH as a substrate observed NO and even N_2O formation during the oxic phase of similar experiments with several AOB strains (Kozlowski *et al.*, 2016; Kozlowski, Kits and Stein, 2016a; Choi, Chaudhry and Martens-Habbena, 2023). These observations, of NO and N_2O formation in the presence of O_2 were again confirmed here (Figure 4). Both substrates (NH_3 or NH_2OH)

can result in the formation of NO and N_2O through abiotic reactions between intermediates, or activity of the HAO, CytL, or CytS enzymes and can therefore result in misidentified NirK or NOR activity. This interference, whether abiotic or biotic, was circumvented here by clearly separating the N_2H_4 injection from the NO_2^- injection, to ensure all NO or N_2O observed originated from an enzymatic denitrification pathway starting with NO_2^-.

As denitrification primarily occurs under O_2 deficiency, verification was needed that no denitrification intermediates were detectable by the sensors during the anoxic phase before the injection of NO_2^-. Surprisingly, however, the NO/N_2O profiles of all three strains differed from each other as soon as anoxia was reached. While high NO concentrations (~400 nM) peaked in *N. multiformis* NI13 soon after anoxia was reached (Figure 5 B), *N. briensis* Nsp1 produced a smaller NO signal (< 50 nM) (Figure 5 C), which was present in varying amounts between the replicates (Figure 5). This contrasted with what was predicted with N_2H_4 being used as the sole electron donor, as no reactive nitrogen species should have been formed through its oxidation. In both strains, the NO signal disappeared entirely after a couple of hours, without the production of measurable N_2O. One explanation for these unexpected NO peaks upon reaching anoxia is that a small amount of NO_2^- was retained by the biomass through the washing process and subsequently reduced by the NirK in each strain to NO. This hypothesis of retained NO_2^- is also supported by NO_2^- measurements taken from the chambers and from biomass that was left to sit for the duration of the MR experiments (Table 3).In contrast to *N. briensis* Nsp1 and *N. multiformis* NI13, *N. europaea* Nm50 did not show any NO signal at anoxia (Figure 5 A). This was particularly interesting because *N. europaea* Nm50 retained by far the most NO_2^- (>15.6 µM) after washing (Table 3).

Although all three strains differed in this first test with N_2H_4 as a substrate, all sensors returned to a steady state and detected no NO/N_2O after a couple of hours. This allowed for the following experiments to be conducted without an introduced NO/N_2O background. In combination with this sensor setup, which can detect O_2, NO, and N_2O simultaneously and in real-time, this was an overall novel approach, which to our knowledge has not been done before.

AOB partial denitrification (NO/N_2O) profiles

The three AOB tested here all possess different NOR genetic repertoires (Table 2). Therefore, it was hypothesized that they would display different NO production (release), NO consumption, and N_2O production profiles when provided an electron donor and NO_2^- in an anoxic environment (Figure 6). This was true for the initial release of NO at anoxia

resulting from retained NO_2^- after washing (mentioned above), and for external NO_2^- injected afterward.

As previous studies have shown, the presence or absence of a cNOR directly impacts the amount of NO released during nitrifier denitrification (Kozlowski, Price and Stein, 2014). However, the sNOR group of enzymes are a recently described subset of NOR enzymes that to date have not had their substrate experimentally verified (Murali *et al.*, 2021; Murali, Hemp and Gennis, 2022). Therefore, it was unclear what the NO and N_2O profile would be in the absence of a canonical cNOR, if an sNOR was present, as is the case for the *N. briensis* Nsp1 strain tested here. Interestingly this *N. briensis* Nsp1 strain again had a different NO release profile compared to *N. europaea* Nm50 and *N. multiformis* NI13*,* forming a middle ground between the profiles of the other two. Most importantly, it did not produce any measurable amount of N_2O. The exception was when NO concentrations exceeded our upper detection limit for several hours and abiotic production of N_2O likely occurred as has been previously shown (Kozlowski *et al.*, 2016). Interestingly, *N. briensis* Nsp1 did remove up to 160 µM NO_2^- from the MR chambers. The NO_2^- was likely all reduced to NO via the NirK, but the ratio of NO measured to NO_2^- reduced was a lot lower than the ratio produced by *N. multiformis* NI13 (Figure 6). This reduced NO accumulation may indicate that *N. briensis* Nsp1 has another way to deal with the NO produced by the NirK, without reducing NO to N_2O. Based on these results the presence of a sNOR enzyme does not seem to confer the ability of an AOB to reduce NO to N_2O. However, the accumulation of NO was also lower in the AOB strains encoding a sNOR, compared to the one without any NOR. If this is indeed the result of the sNOR enzyme remains to be seen.

The large differences in the NO/N_2O profiles between the three AOB tested in this study are easiest to compare when a fixed amount of 10 µM NO_2^- was injected into the MR chambers (Figure 6 A, E, I). Here, the NO concentration in *N. multiformis* NI13 increased beyond the upper calibration limit (524 nM). However, *N. briensis* Nsp1 only produced 71.6 nM NO. This variation in NO production per NO_2^- injected between these two AOB was consistent when injecting higher amounts of NO_2^- concentrations (Figure 6 B-D, F-H, J-L). One replicate of each *N. briensis* Nsp1 and *N. multiformis* NI13 produced a stable amount of N_2O. In these instances, the immediate formation of NO upon NO_2^- injection vastly exceeded the upper detection limit (524 nM) of the NO sensor. Thus, abiotic denitrification is likely to have occurred. Another possibility is that denitrification through the CytS may be activated at these high NO_2^- concentrations (Elmore *et al.*, 2007; Klotz and Stein, 2008; Caranto, Vilbert and Lancaster, 2016). Both *N. briensis* Nsp1 and *N. multiformis* NI13 would have the necessary gene repertoire (Table 2). In the case of *N. briensis* Nsp1 N_2O production by CytL

or the sNOR with these high NO concentrations cannot be fully excluded but is highly unlikely based on the other replicates and *N. multiformis* NI13 also producing abiotic N_2O in high NO concentrations without either one of these enzymes.

In contrast to what was observed with *N. briensis* Nsp1 and *N. multiformis* NI13, *N. europaea* Nm50 was able to denitrify NO_2^- to N_2O. Regardless of the amount of NO_2^- injected, no measurable NO accumulation was observed. However, it should be noted that in each case the amount of N_2O formed was not stoichiometric to the amount of NO_2^- injected, regardless of the NO_2^- concentration injected. It is possible that during denitrification, the more volatile NO may have reacted with compounds in the medium or biotic cellular products making it unavailable for further reduction. As the NO concentration never increases in the MR chambers, this suggests that all the NO produced by the present NirK is used up immediately. Thus, the NirK likely is the rate limiting enzyme in this pathway. While denitrification by *N. europaea* Nm50 was an expected result (Beaumont *et al.*, 2002, 2004; Cantera and Stein, 2007; Yu and Chandran, 2010; Yu *et al.*, 2010; Kozlowski, Price and Stein, 2014), this positive control highlights how stable N_2O is once formed in this MR chamber setup.

N. europaea Nm50 denitrification kinetics

N. europaea Nm50 was the sole AOB tested in this study that was able to carry out nitrifier denitrification, producing stable amounts of N_2O from NO_2^- under anoxic conditions (Figure 6). Interestingly, the N_2O concentrations produced by *N. europaea* Nm50 did not represent a 1:1 stoichiometric conversion of NO_2^- injected to N_2O produced. This was true even when accounting for NO_2^- that may have been carried over into the experiment (mentioned above). Again, it is likely that some of the NO reacted with the medium or was lost in another fashion before the cNOR could further reduce it. This is even more likely given the long duration of the experiment due to the time it takes for the biomass to go through the injected NO_2^-. Nevertheless, the only obvious biotic denitrification during this study was observed in *N. europaea* Nm50. This further supports previous studies regarding the need for the cNOR to perform denitrification (Kozlowski, Price and Stein, 2014; Kozlowski, Kits and Stein, 2016a). Previous experiments done on *N. europaea* ATCC 19718 with N_2H_4 and 2 mM NO_2^- injections also showed very similar NO and N_2O profiles (Kozlowski, Price and Stein, 2014). Whole cell kinetic experiments looking at the whole denitrification pathway in *N. europaea* Nm50 revealed that N_2O is indeed produced enzymatically (Figure 7). As NO production by NirK seems to be the rate limiting enzymatic step it is not possible to estimate the maximal rate of NO reduction by the cNOR itself from the available data. In addition, due to the high variation in the V_{max} after normalization to whole chamber protein concentrations, it was not

possible to report a single definite V_{max} value. This is likely a result of the accumulation of inactive biomass in the culture, resulting in an overestimation of the active protein concentration in the samples and therefore biasing the normalization. In the future, it would be advantageous to harvest biomass from a fresh culture in its exponential growth phase to minimize this bias. Also, while the biomass was grown on its natural substrate (NH_4Cl), these experiments were performed with an alternative electron donor (N_2H_4) and the addition of NO_2^- afterward, which should be taken into account when comparing the $K_{m(app)}$ and V_{max} values reported here. With these caveats in mind, this was to the author's best knowledge still the first attempt to model denitrification kinetics in an AOB.

It is important to note that the whole cell denitrification pathway of *N. europaea* Nm50 measured here has multiple enzymatic steps and may also rely on the transport of NO_2^- or the diffusion of NO. To this end, NO remained under the detection limit during all kinetic measurements reported here. Interestingly, at very high NO_2^- concentrations (>4 mM), NO concentrations did become detectable in the MR chambers (Figure 8). However, these data points were not considered when calculating the denitrification kinetic constants of *N. europaea* Nm50.

NO is removed from the chamber but not converted to N_2O

Although some of the *N. europaea* Nm50 replicates were very close, it was not possible to produce a consistent stoichiometric conversion of NO_2^- to N_2O. In addition, it was confirmed with a nitrite assay that either no or very little NO_2^- was left in the chamber at the end of each experiment, ruling out that *N. europaea* Nm50 was unable to reduce all the NO_2^- provided. The initially injected NO_2^- had to be transformed along the denitrification pathway, most likely from NO, as it is the most reactive and volatile intermediate. This inherent loss of reactive nitrogen during the denitrification pathway makes it hard to prove stoichiometric conversion in this experimental setup. This is reflected in all three strains, where NO is produced (in *N. europaea* Nm50 immediately converted to N_2O) but disappears over time. NO_2^- measurements from the MR experiments showed that at the end of each run with *N. briensis* Nsp1 and *N. multiformis* NI13, all the NO_2^- injected had been transformed. Hence, both strains were able to reduce all the NO_2^- injected but did not produce any N_2O. Preliminary data of endpoint measurements from the MR chambers suggests that NH_3 or NH_4^+ is formed during the experiments. NO and N_2H_4 have been shown to react with each other in various ways under certain conditions (Sawyer and Glassman, 1967; Cho and Chang, 1997). Preliminary data of endpoint measurements from the MR chambers indicates that NH_3 or NH_4^+ is formed during the experiments. NO and N_2H_4 have been shown to react with each other in various ways under certain conditions.

N. multiformis NI13 might be a good starting point in the future to investigate the fate of, if not being reduced to N_2O. *N. multiformis* NI13 denitrifies the NO_2^- to NO through its NirK but can't further convert it to N_2O due to the lack of NORs. This results in very high amounts of NO released even when small concentrations of NO_2^- are injected. N-labeling and endpoint measurements of N-species could be employed to investigate the fate of the NO produced by the NirK. Both can be combined with the chemical assays used here and gas chromatography (GC) or membrane-inlet mass spectrometry (MIMS) as an alternative measurement method.

Study limitations and the future of studying nitrifier denitrification

Some of the open questions left to be addressed through the MR method presented here remain. One of the major limitations in revealing stoichiometric conversion rates and where NO binds to was the detection limit of the NO sensor used. In many of the experiments performed and shown here, the upper detection limit of the NO sensor was surpassed. In combination with how the AOB reacted so differently in their NO release profile, it was not possible to consistently quantify NO production. The theoretical detection limit of the sensor used here is 3 µM NO. This could likely be reached with other calibration methods like NO gas in a sealed vial under anoxic conditions. Due to the duration and amount of the experiments performed in this study, it was not feasible to use something other than the NO donor calibration used here, which was done under oxic conditions in the same MR chamber where all experiments took place. While this method gave a good sensitivity (< 5 nM) it also restricted the upper calibration limit at 524 nM NO. Measurements within a higher detection limit would enable us to calculate NO production rates over time and visualize the turning point where NO production ceases. Thus, the calculation of the total amount of NO produced to the amount of NO_2^- injected and N_2O produced is possible and could clarify where stoichiometric conversion occurs and where NO is lost to a different reaction.

A second drawback of this experimental sensor setup is the cross-sensitivity of the N_2O sensor to the NO present in the MR chamber. This cross-sensitivity is why *N. multiformis* NI13 displayed a temporary N_2O signal peak when NO concentrations were above the detection limit, as high NO concentrations led to interference in the N_2O readout. Therefore, only a stable N_2O concentration in the absence of NO can be regarded as reliable N_2O measurements. However, it is an additional confirmation of the presence of NO which is produced at anoxia in *N. multiformis* NI13 and *N. briensis* Nsp1 because the NO sensor signal coincides with the cross-interference signal of the N_2O sensor (see above). NO also disappears again at a similar rate, while no stable amount of N_2O is produced. While this did not affect the results of any experiments looking at the NO and N_2O dynamics in these

three strains, it was a limitation for the kinetic measurements with *N. europaea* Nm50. As NO would sometimes become detectable during these experiments cross-interference signal in the N_2O sensor could not be excluded. If this cross-interference could be circumvented in the future, higher amounts of NO_2^- could also be injected in a kinetic analysis in a similar setup and show potential substrate inhibition of the denitrification pathway.

All three AOB showed distinct NO/N_2O profiles during nitrifier denitrification and parts of them can be explained by their genetic repertoire. Future studies should focus on expanding the amount and variation of AOB strains in a similar setup. For example, what would the nitrifier denitrification profile of an AOB like *Nitrosomonas sp.* 41 Nm58 that does not encode a NirK look like? Additionally, while the results presented here were reproducible within the same strain it was not possible to expand further into different strains with the same genetic makeup. For example, comparing *N. europaea* Nm50 to *N. briensis* Nsp8, both having a cNOR and sNOR. Would they show the same NO/N_2O profile even though they belong to different genera?

CONCLUSION

The combination of N_2H_4 as an alternative electron donor and an MR chamber experimental setup, where O_2, NO, and N_2O can be simultaneously measured allowed for novel insights into the nitrifier denitrification pathway of several AOB species. No denitrification capabilities of the sNOR could be determined, which further supports the hypothesis that this enzyme has a different function than being a NOR. This also means that the sNOR should not be used as a marker gene for the denitrification pathway in metagenomic analyses. *N. europaea* Nm50 was the only AOB in this study that was able to enzymatically produce N_2O. This is in line with previous studies, where a cNOR was deemed necessary for the biotic conversion of NO to N_2O in AOB. Although no enzymatic N_2O production was observed with the other strains the results clearly showed that NO is always produced by the NirK but reacts either biotically or abiotically to something other than N_2O. This was the case for both *N. briensis* Nsp1 and *N. multiformis* NI13 as long as the initial NO_2^- concentrations injected were below 50 µM. Together, this indicates that AOB in general contribute to the biotic and abiotic formation of global N_2O emissions and can remove large amounts of NO_2^- in anoxic environments. One, however, must acknowledge the use of N_2H_4 and the general laboratory conditions make it harder to extrapolate from these results to the denitrification behavior or rates of AOB in the environment. In conclusion, this method can be applied to several other nitrifying and denitrifying microorganisms to further improve our understanding of the enzymes involved in the denitrification pathway and their contribution to abiotic and biotic N_2O emissions.

Consumables

Table 4: Consumables used in this study.

Consumable	Manufacturer
0.2 µm PES bottle top filter	Avantor
96 well plates, flat bottom, transparent	Greiner
Eppendorf tubes, various sizes	Eppendorf
Glass bottles, screwcap, various sizes	Schott
Glass coated magnets	Unisense
Hamilton syringe (10 µL and 500 µL)	Hamilton
PCR film, adhesive	Eppendorf
Serological pipettes, sterile, single use, various sizes	
SPADBAS (Basic spot adapter)	PyroScience
SPGLUE (silicone glue)	PyroScience
Sterican needles, sterile, various sizes	Roth
Tips, various sizes, with and without filter	Biozym
TROXSP5 (trace range oxygen sensor spots)	PyroScience
Ultra-15 Centrifugal Filter Units (14,000 kDa cut off)	Amicon

Equipment

Table 5: Equipment used in this study.

Equipment	Manufacturer
Balance (BL3100)	Sartorius
Centrifuge 5804R, A-4-44 and FA 45-30-11 rotors	Eppendorf
Eppendorf Research Pipettes, various sizes	Eppendorf
FireSting-GO2 (pocket oxygen meter)	PyroScience
FireSting-PRO (optical pH & oxygen & temperature meter)	PyroScience
GFL 1004 water bath	GFL
Hanna HI-series (ph-meter)	Hanna Instruments
Infinite M200 PRO multimode microplate reader	Tecan
Laminar flow (Savvy Class II)	Lamsystems
MicroRespiration glass chamber (2 mL and 10 mL) with glass lids	Unisense
MicroRespiration Rack (MR2-Rack)	Unisense
MicroRespiration Stirrer controller (MR2-Co)	Unisense
N_2O-MR, tip diameter: 500 µm (electrochemical microsensors)	Unisense
NO-MR, tip diameter: 500 µm (electrochemical microsensors)	Unisense
Pipetboy acu 2 (pipette controller)	Integra Biosciences
SAFEVAC Vacuum Aspiration systems	DLAB
SPFIB-LNS (optical fiber withlLens)	PyroScience
UniAmp Multi Channel (microsensor amplifier)	Unisense
Vacusafe Comfort Aspiration system	Integra Biosciences

Kits

Table 6: Kits used in this study.

Kit	Manufacturer
BCA Protein Assay Kit	Pierce
N_2O Sensor Calibration Kit	Unisense
SPGLUE-KIT (Gluing Kit)	PyroScience

Abbreviations

Table 7: Abbreviations used in this thesis.

Abbreviation	
aa3	Low-affinity heme-copper-containing terminal oxidase (A1 type)
AMO	Ammonia monooxygenase
Anammox	Anaerobic ammonium oxidation
AOA	Ammonia-oxidizing archaea
AOB	Ammonia-oxidizing bacteria
BCA	Bicinchoninic acid
bo3	Quinol-oxidizing terminal oxidase
cbb3	High-affinity heme-copper-containing terminal oxidase (C type)
CH_4	Methane
cNOR	Canonical heme-iron-containing nitric oxide reductase
Comammox	Complete ammonia oxidation
CO_2	Carbon dioxide
CytL	C-type cytochrome P460
CytS	C-type cytochrome c′-beta
HAO	Hydroxylamine dehydrogenase
HCl	Hydrochloric acid
HCO	Heme-copper-oxidase
HEPES	4-(2-hydroxyethyl)-1-piperazineethanesulfonic acid
$K_{m(app)}$	Apparent substrate affinity
LB	Lysogeny broth
MQ	Milli-Q
MR	Microrespiration
N_2	Dinitrogen
N_2H_4	Hydrazine
N_2O	Nitrous oxide
NaCl	Sodium chloride
$NaHCO_3$	Sodium bicarbonate
NaOH	Sodium hydroxide
NcyA	Nitrosocyanin
NEDD	N-naphthyl ethylenediamine dihydrochloride
NH_2OH	Hydroxylamine
NH_3	Ammonia
NH_4^+	Ammonium
NH_4Cl	Ammonium chloride

NH_4NO_3	Ammonium nitrate
$(NH_4)_2SO_4$	Ammonium sulfate
NirK	Nitrite reductase
NO	Nitric oxide
NO_2^-	Nitrite
NO_3^-	Nitrate
NOB	Nitrite-oxidizing bacteria
NOO	Nitric oxide oxidoreductase
NOR	Nitric oxide reductase
NO_x	Nitrogen oxides
NsrR	NO-responsive transcriptional regulator R
NsrS	NO-responsive transcriptional regulator S
Nxr	Nitrite oxidoreductase
O_2	Dioxygen
PES	Polyethersulfone
qPCR	Quantitative polymerase chain reaction
rRNA	Ribosomal ribonucleic acid
SD	Standard deviation
sNOR	Putative heme-copper-containing nitric oxide reductase
VCl_3	Vanadium(III) chloride
V_{max}	maximum velocity of an enzymatic reaction
WWTPs	Wastewater treatment plants

References

Agogué, H. *et al.* (2008) 'Major gradients in putatively nitrifying and non-nitrifying Archaea in the deep North Atlantic', *Nature*, 456(7223), pp. 788–791.

Anderson, I.C. *et al.* (1993) 'A comparison of NO and N2O production by the autotrophic nitrifier Nitrosomonas europaea and the heterotrophic nitrifier Alcaligenes faecalis', *Applied and Environmental Microbiology*, 59(11), pp. 3525–3533. Available at: https://doi.org/10.1128/aem.59.11.3525-3533.1993.

Arciero, D.M. *et al.* (2002) 'Nitrosocyanin, a Red Cupredoxin-like Protein from *Nitrosomonas europaea*', *Biochemistry*, 41(6), pp. 1703–1709. Available at: https://doi.org/10.1021/bi015908w.

Arp, D.J. and Stein, L.Y. (2003) 'Metabolism of inorganic N compounds by ammonia-oxidizing bacteria', *Critical Reviews in Biochemistry and Molecular Biology*, 38(6), pp. 471–495.

Beaumont, H.J.E. *et al.* (2002) 'Nitrite Reductase of *Nitrosomonas europaea* Is Not Essential for Production of Gaseous Nitrogen Oxides and Confers Tolerance to Nitrite', *Journal of Bacteriology*, 184(9), pp. 2557–2560. Available at: https://doi.org/10.1128/JB.184.9.2557-2560.2002.

Beaumont, H.J.E. *et al.* (2004) '*Nitrosomonas europaea* Expresses a Nitric Oxide Reductase during Nitrification', *Journal of Bacteriology*, 186(13), pp. 4417–4421. Available at: https://doi.org/10.1128/JB.186.13.4417-4421.2004.

Beman, J.M., Sachdeva, R. and Fuhrman, J.A. (2010) 'Population ecology of nitrifying Archaea and Bacteria in the Southern California Bight', *Environmental Microbiology*, 12(5), pp. 1282–1292.

Blainey, P.C. *et al.* (2011) 'Genome of a Low-Salinity Ammonia-Oxidizing Archaeon Determined by Single-Cell and Metagenomic Analysis', *PLoS ONE*. Edited by J. Gilbert, 6(2), p. e16626. Available at: https://doi.org/10.1371/journal.pone.0016626.

Bobbink, R. *et al.* (2010) 'Global assessment of nitrogen deposition effects on terrestrial plant diversity: a synthesis', *Ecological applications*, 20(1), pp. 30–59.

Bollmann, A. *et al.* (2013) 'Complete genome sequence of Nitrosomonas sp. Is79, an ammonia oxidizing bacterium adapted to low ammonium concentrations', *Standards in Genomic Sciences*, 7(3), pp. 469–482. Available at: https://doi.org/10.4056/sigs.3517166.

Cantera, J.J.L. and Stein, L.Y. (2007) 'Role of nitrite reductase in the ammonia-oxidizing pathway of Nitrosomonas europaea', *Archives of Microbiology*, 188(4), pp. 349–354. Available at: https://doi.org/10.1007/s00203-007-0255-4.

Caranto, J.D. and Lancaster, K.M. (2017) 'Nitric oxide is an obligate bacterial nitrification intermediate produced by hydroxylamine oxidoreductase', *Proceedings of the National Academy of Sciences*, 114(31), pp. 8217–8222. Available at: https://doi.org/10.1073/pnas.1704504114.

Caranto, J.D., Vilbert, A.C. and Lancaster, K.M. (2016) '*Nitrosomonas europaea* cytochrome P460 is a direct link between nitrification and nitrous oxide emission', *Proceedings of the National Academy of Sciences*, 113(51), pp. 14704–14709. Available at: https://doi.org/10.1073/pnas.1611051113.

Cho, C.M.-H. *et al.* (2006) 'Transcriptome of a Nitrosomonas europaea Mutant with a Disrupted Nitrite Reductase Gene (nirK)', *Applied and Environmental Microbiology*, 72(6), pp. 4450–4454. Available at: https://doi.org/10.1128/AEM.02958-05.

Cho, Y.-H. and Chang, H.-M. (1997) 'A kinetic model for the reduction of nitric oxide by hydrazine', *KSME International Journal*, 11(4), pp. 428–434. Available at: https://doi.org/10.1007/BF02945081.

Choi, E., Chaudhry, S.I. and Martens-Habbena, W. (2023) 'Role of Nitric Oxide in Hydroxylamine Oxidation by Ammonia-Oxidizing Bacteria', *Applied and Environmental Microbiology*. Edited by I. Cann, pp. e02173-22. Available at: https://doi.org/10.1128/aem.02173-22.

Clark, L.C. *et al.* (1953) '*Continuous Recording of Blood Oxygen Tensions by Polarography*', *Journal of Applied Physiology*, 6(3), pp. 189–193. Available at: https://doi.org/10.1152/jappl.1953.6.3.189.

Daims, H. *et al.* (2015) 'Complete nitrification by Nitrospira bacteria', *Nature*, 528(7583), pp. 504–509. Available at: https://doi.org/10.1038/nature16461.

De Vries, W. *et al.* (2013) 'Assessing planetary and regional nitrogen boundaries related to food security and adverse environmental impacts', *Current Opinion in Environmental Sustainability*, 5(3–4), pp. 392–402. Available at: https://doi.org/10.1016/j.cosust.2013.07.004.

Di, H.J. *et al.* (2009) 'Nitrification driven by bacteria and not archaea in nitrogen-rich grassland soils', *Nature Geoscience*, 2(9), pp. 621–624.

Elmore, B.O. *et al.* (2007) 'Cytochromes P460 and *c '*-beta; A new family of high-spin cytochromes *c*', *FEBS Letters*, 581(5), pp. 911–916. Available at: https://doi.org/10.1016/j.febslet.2007.01.068.

Erisman, J.W. *et al.* (2008) 'How a century of ammonia synthesis changed the world', *Nature geoscience*, 1(10), pp. 636–639.

Erisman, J.W. *et al.* (2011) 'Reactive nitrogen in the environment and its effect on climate change', *Current Opinion in Environmental Sustainability*, 3(5), pp. 281–290. Available at: https://doi.org/10.1016/j.cosust.2011.08.012.

Erisman, J.W. *et al.* (2013) 'Consequences of human modification of the global nitrogen cycle', *Philosophical Transactions of the Royal Society B: Biological Sciences*, 368(1621), p. 20130116. Available at: https://doi.org/10.1098/rstb.2013.0116.

Erisman, J.W. and Larsen, T.A. (2013) 'Nitrogen economy of the 21st century', *Source separation and decentralization for wastewater management*, pp. 45–58.

Francis, C.A. *et al.* (2005) 'Ubiquity and diversity of ammonia-oxidizing archaea in water columns and sediments of the ocean', *Proceedings of the National Academy of Sciences*, 102(41), pp. 14683–14688. Available at: https://doi.org/10.1073/pnas.0506625102.

Füssel, J. *et al.* (2017) 'Adaptability as the key to success for the ubiquitous marine nitrite oxidizer *Nitrococcus*', *Science Advances*, 3(11), p. e1700807. Available at: https://doi.org/10.1126/sciadv.1700807.

García-Robledo, E., Corzo, A. and Papaspyrou, S. (2014) ‘A fast and direct spectrophotometric method for the sequential determination of nitrate and nitrite at low concentrations in small volumes’, *Marine Chemistry*, 162, pp. 30–36. Available at: https://doi.org/10.1016/j.marchem.2014.03.002.

Giuffrè, A. *et al.* (1999) ‘The heme-copper oxidases of *Thermus thermophilus* catalyze the reduction of nitric oxide: Evolutionary implications’, *Proceedings of the National Academy of Sciences*, 96(26), pp. 14718–14723. Available at: https://doi.org/10.1073/pnas.96.26.14718.

van de Graaf, A.A. *et al.* (1995) ‘Anaerobic oxidation of ammonium is a biologically mediated process’, *Applied and Environmental Microbiology*, 61(4), pp. 1246–1251. Available at: https://doi.org/10.1128/aem.61.4.1246-1251.1995.

Griffis, T.J. *et al.* (2017) ‘Nitrous oxide emissions are enhanced in a warmer and wetter world’, *Proceedings of the National Academy of Sciences*, 114(45), pp. 12081–12085. Available at: https://doi.org/10.1073/pnas.1704552114.

Hall, B.D., Dutton, G.S. and Elkins, J.W. (2007) ‘The NOAA nitrous oxide standard scale for atmospheric observations’, *Journal of Geophysical Research: Atmospheres*, 112(D9). Available at: https://doi.org/10.1029/2006JD007954.

Hallam, S.J. *et al.* (2006) ‘Genomic analysis of the uncultivated marine crenarchaeote *Cenarchaeum symbiosum*’, *Proceedings of the National Academy of Sciences*, 103(48), pp. 18296–18301. Available at: https://doi.org/10.1073/pnas.0608549103.

Han, P. *et al.* (2021) ‘N2O and NOy production by the comammox bacterium Nitrospira inopinata in comparison with canonical ammonia oxidizers’, *Water Research*, 190, p. 116728. Available at: https://doi.org/10.1016/j.watres.2020.116728.

Herrmann, M., Saunders, A.M. and Schramm, A. (2009) ‘Effect of lake trophic status and rooted macrophytes on community composition and abundance of ammonia-oxidizing prokaryotes in freshwater sediments’, *Applied and Environmental Microbiology*, 75(10), pp. 3127–3136.

Hollocher, T.C., Tate, M.E. and Nicholas, D.J. (1981) ‘Oxidation of ammonia by Nitrosomonas europaea. Definite 18O-tracer evidence that hydroxylamine formation involves a monooxygenase.’, *Journal of Biological Chemistry*, 256(21), pp. 10834–10836. Available at: https://doi.org/10.1016/S0021-9258(19)68518-2.

Hommes, N., Sayavedra-Soto, L. and Arp, D. (2002) ‘The roles of the three gene copies encoding hydroxylamine oxidoreductase in Nitrosomonas europaea’, *Archives of Microbiology*, 178(6), pp. 471–476. Available at: https://doi.org/10.1007/s00203-002-0477-4.

Hooper, A. (1978) ‘Nitrogen oxidation and electron transport in ammonia-oxidizing bacteria’, *Microbiology*, pp. 299–304.

Hooper, A.B. (1968) ‘A nitrite-reducing enzyme from Nitrosomonas europaea Preliminary characterization with hydroxylamine as electron donor’, *Biochimica et Biophysica Acta (BBA) - Bioenergetics*, 162(1), pp. 49–65. Available at: https://doi.org/10.1016/0005-2728(68)90213-2.

Hooper, A.B. *et al.* (2005) ‘The oxidation of ammonia as an energy source in bacteria’, *Respiration in archaea and bacteria*, 2, pp. 121–147.

Hooper, A.B., Maxwell, P.C. and Terry, K.R. (1978) 'Hydroxylamine oxidoreductase from Nitrosomonas: absorption spectra and content of heme and metal', *Biochemistry*, 17(15), pp. 2984–2989. Available at: https://doi.org/10.1021/bi00608a007.

Hooper, A.B. and Terry, K.R. (1977) 'Hydroxylamine oxidoreductase from Nitrosomonas: inactivation by hydrogen peroxide', *Biochemistry*, 16(3), pp. 455–459. Available at: https://doi.org/10.1021/bi00622a018.

Hooper, A.B. and Terry, K.R. (1979) 'Hydroxylamine oxidoreductase of Nitrosomonas', *Biochimica et Biophysica Acta (BBA) - Enzymology*, 571(1), pp. 12–20. Available at: https://doi.org/10.1016/0005-2744(79)90220-1.

Hooper, A.B., Terry, K.R. and Maxwell, P.C. (1977) 'Hydroxylamine oxidoreductase of Nitrosomonas. Oxidation of diethyldithiocarbamate concomitant with stimulation of nitrite synthesis', *Biochimica et Biophysica Acta (BBA) - Bioenergetics*, 462(1), pp. 141–152. Available at: https://doi.org/10.1016/0005-2728(77)90196-7.

Jetten, M.S. *et al.* (2001) 'Microbiology and application of the anaerobic ammonium oxidation ("anammox") process', *Current opinion in biotechnology*, 12(3), pp. 283–288.

Jetten, M.S., Horn, S.J. and van Loosdrecht, M.C. (1997) 'Towards a more sustainable municipal wastewater treatment system', *Water science and technology*, 35(9), pp. 171–180.

Jia, Z. and Conrad, R. (2009) 'Bacteria rather than Archaea dominate microbial ammonia oxidation in an agricultural soil', *Environmental Microbiology*, 11(7), pp. 1658–1671. Available at: https://doi.org/10.1111/j.1462-2920.2009.01891.x.

Jones, L.C. *et al.* (2015) 'Stable Isotopes and Iron Oxide Mineral Products as Markers of Chemodenitrification.', *Environmental Science & Technology*, 49(6), pp. 3444–3452. Available at: https://doi.org/10.1021/es504862x.

Jung, M.-Y. *et al.* (2019) 'Indications for enzymatic denitrification to N2O at low pH in an ammonia-oxidizing archaeon', *The ISME Journal*, 13(10), pp. 2633–2638. Available at: https://doi.org/10.1038/s41396-019-0460-6.

Karner, M.B., DeLong, E.F. and Karl, D.M. (2001) 'Archaeal dominance in the mesopelagic zone of the Pacific Ocean', *Nature*, 409(6819), pp. 507–510.

Kartal, B. *et al.* (2007) 'Anammox bacteria disguised as denitrifiers: nitrate reduction to dinitrogen gas via nitrite and ammonium', *Environmental Microbiology*, 9(3), pp. 635–642. Available at: https://doi.org/10.1111/j.1462-2920.2006.01183.x.

Ke, X., Lu, W. and Conrad, R. (2015) 'High Oxygen Concentration Increases the Abundance and Activity of Bacterial Rather than Archaeal Nitrifiers in Rice Field Soil', *Microbial Ecology*, 70(4), pp. 961–970. Available at: https://doi.org/10.1007/s00248-015-0633-4.

van Kessel, M.A.H.J. *et al.* (2015) 'Complete nitrification by a single microorganism', *Nature*, 528(7583), pp. 555–559. Available at: https://doi.org/10.1038/nature16459.

Kim, B.K. *et al.* (2011) 'Genome Sequence of an Ammonia-Oxidizing Soil Archaeon, "Candidatus Nitrosoarchaeum koreensis" MY1', *Journal of Bacteriology*, 193(19), pp. 5539–5540. Available at: https://doi.org/10.1128/JB.05717-11.

Kits, K.D. *et al.* (2017) ‘Kinetic analysis of a complete nitrifier reveals an oligotrophic lifestyle’, *Nature*, 549(7671), pp. 269–272. Available at: https://doi.org/10.1038/nature23679.

Kits, K.D. *et al.* (2019) ‘Low yield and abiotic origin of N2O formed by the complete nitrifier Nitrospira inopinata’, *Nature Communications*, 10(1), p. 1836. Available at: https://doi.org/10.1038/s41467-019-09790-x.

Klotz, M.G. *et al.* (2006) ‘Complete Genome Sequence of the Marine, Chemolithoautotrophic, Ammonia-Oxidizing Bacterium Nitrosococcus oceani ATCC 19707’, *Applied and Environmental Microbiology*, 72(9), pp. 6299–6315. Available at: https://doi.org/10.1128/AEM.00463-06.

Klotz, M.G. and Stein, L.Y. (2008) ‘Nitrifier genomics and evolution of the nitrogen cycle’, *FEMS Microbiology Letters*, 278(2), pp. 146–156. Available at: https://doi.org/10.1111/j.1574-6968.2007.00970.x.

Könneke, M. *et al.* (2005) ‘Isolation of an autotrophic ammonia-oxidizing marine archaeon’, *Nature*, 437(7058), pp. 543–546. Available at: https://doi.org/10.1038/nature03911.

Kozlowski, J.A. *et al.* (2016) ‘Pathways and key intermediates required for obligate aerobic ammonia-dependent chemolithotrophy in bacteria and Thaumarchaeota’, *The ISME Journal*, 10(8), pp. 1836–1845. Available at: https://doi.org/10.1038/ismej.2016.2.

Kozlowski, J.A., Kits, K.D. and Stein, L.Y. (2016a) ‘Comparison of Nitrogen Oxide Metabolism among Diverse Ammonia-Oxidizing Bacteria’, *Frontiers in Microbiology*, 7. Available at: https://doi.org/10.3389/fmicb.2016.01090.

Kozlowski, J.A., Kits, K.D. and Stein, L.Y. (2016b) ‘Genome Sequence of Nitrosomonas communis Strain Nm2, a Mesophilic Ammonia-Oxidizing Bacterium Isolated from Mediterranean Soil’, *Genome Announcements*, 4(1), pp. e01541-15. Available at: https://doi.org/10.1128/genomeA.01541-15.

Kozlowski, J.A., Price, J. and Stein, L.Y. (2014) ‘Revision of N2O-Producing Pathways in the Ammonia-Oxidizing Bacterium Nitrosomonas europaea ATCC 19718’, *Applied and Environmental Microbiology*. Edited by R.E. Parales, 80(16), pp. 4930–4935. Available at: https://doi.org/10.1128/AEM.01061-14.

Kraft, B. *et al.* (2022) ‘Oxygen and nitrogen production by an ammonia-oxidizing archaeon’, *Science*, 375(6576), pp. 97–100. Available at: https://doi.org/10.1126/science.abe6733.

Lancaster, K.M. *et al.* (2018) ‘Alternative Bioenergy: Updates to and Challenges in Nitrification Metalloenzymology’, *Joule*, 2(3), pp. 421–441. Available at: https://doi.org/10.1016/j.joule.2018.01.018.

Leininger, S. *et al.* (2006) ‘Archaea predominate among ammonia-oxidizing prokaryotes in soils’, *Nature*, 442(7104), pp. 806–809.

Liu, S. *et al.* (2017) ‘Abiotic Conversion of Extracellular NH_2OH Contributes to N_2O Emission during Ammonia Oxidation’, *Environmental Science & Technology*, 51(22), pp. 13122–13132. Available at: https://doi.org/10.1021/acs.est.7b02360.

Martens-Habbena, W. *et al.* (2015) ‘The production of nitric oxide by marine ammonia-oxidizing archaea and inhibition of archaeal ammonia oxidation by a nitric oxide scavenger’,

Environmental Microbiology, 17(7), pp. 2261–2274. Available at: https://doi.org/10.1111/1462-2920.12677.

Matsuda, Y. *et al.* (2002) 'Nitric Oxide-Reductase Homologue That Contains a Copper Atom and Has Cytochrome c-Oxidase Activity from an Aerobic Phototrophic Bacterium Roseobacter denitrificans', *Journal of Biochemistry*, 131(6), pp. 791–800. Available at: https://doi.org/10.1093/oxfordjournals.jbchem.a003167.

Mellbye, B.L. *et al.* (2018) 'Genome-Scale, Constraint-Based Modeling of Nitrogen Oxide Fluxes during Coculture of Nitrosomonas europaea and Nitrobacter winogradskyi', *mSystems*, 3(3), p. 10.1128/msystems.00170-17. Available at: https://doi.org/10.1128/msystems.00170-17.

Mincer, T.J. *et al.* (2007) 'Quantitative distribution of presumptive archaeal and bacterial nitrifiers in Monterey Bay and the North Pacific Subtropical Gyre', *Environmental microbiology*, 9(5), pp. 1162–1175.

Miranda, K.M., Espey, M.G. and Wink, D.A. (2001) 'A Rapid, Simple Spectrophotometric Method for Simultaneous Detection of Nitrate and Nitrite', *Nitric Oxide*, 5(1), pp. 62–71. Available at: https://doi.org/10.1006/niox.2000.0319.

Murali, R. *et al.* (2021) *Diversity and evolution of nitric oxide reduction*. preprint. Biochemistry. Available at: https://doi.org/10.1101/2021.10.15.464467.

Murali, R., Hemp, J. and Gennis, R.B. (2022) 'Evolution of quinol oxidation within the heme-copper oxidoreductase superfamily', *Biochimica et Biophysica Acta (BBA) - Bioenergetics*, 1863(8), p. 148907. Available at: https://doi.org/10.1016/j.bbabio.2022.148907.

Norton, J.M. *et al.* (2008) 'Complete Genome Sequence of *Nitrosospira multiformis* , an Ammonia-Oxidizing Bacterium from the Soil Environment', *Applied and Environmental Microbiology*, 74(11), pp. 3559–3572. Available at: https://doi.org/10.1128/AEM.02722-07.

Palomo, A. *et al.* (2016) 'Metagenomic analysis of rapid gravity sand filter microbial communities suggests novel physiology of Nitrospira spp.', *The ISME journal*, 10(11), pp. 2569–2581.

Pärn, J. *et al.* (2018) 'Nitrogen-rich organic soils under warm well-drained conditions are global nitrous oxide emission hotspots', *Nature Communications*, 9(1), p. 1135. Available at: https://doi.org/10.1038/s41467-018-03540-1.

Payne, R.J. *et al.* (2013) 'Impact of nitrogen deposition at the species level', *Proceedings of the National Academy of Sciences*, 110(3), pp. 984–987.

Pinto, A.J. *et al.* (2016) 'Metagenomic evidence for the presence of comammox Nitrospira-like bacteria in a drinking water system', *Msphere*, 1(1), pp. 10–1128.

Poth, M. and Focht, D.D. (1985) '^{15} N Kinetic Analysis of N_2O Production by *Nitrosomonas europaea* : an Examination of Nitrifier Denitrification', *Applied and Environmental Microbiology*, 49(5), pp. 1134–1141. Available at: https://doi.org/10.1128/aem.49.5.1134-1141.1985.

Prather, M.J. *et al.* (2015) 'Measuring and modeling the lifetime of nitrous oxide including its variability', *Journal of Geophysical Research: Atmospheres*, 120(11), pp. 5693–5705. Available at: https://doi.org/10.1002/2015JD023267.

Prinn, R.G. *et al.* (2018) 'History of chemically and radiatively important atmospheric gases from the Advanced Global Atmospheric Gases Experiment (AGAGE)', *Earth System Science Data*, 10(2), pp. 985–1018. Available at: https://doi.org/10.5194/essd-10-985-2018.

Prosser, J.I. and Nicol, G.W. (2008) 'Relative contributions of archaea and bacteria to aerobic ammonia oxidation in the environment', *Environmental microbiology*, 10(11), pp. 2931–2941.

Purkhold, U. *et al.* (2000) 'Phylogeny of all recognized species of ammonia oxidizers based on comparative 16S rRNA and amoA sequence analysis: implications for molecular diversity surveys', *Applied and environmental microbiology*, 66(12), pp. 5368–5382.

Richardson, K. *et al.* (2023) 'Earth beyond six of nine planetary boundaries', *Science Advances*, 9(37), p. eadh2458. Available at: https://doi.org/10.1126/sciadv.adh2458.

Rockström, J. *et al.* (2009) 'A safe operating space for humanity', *Nature*, 461(7263), pp. 472–475. Available at: https://doi.org/10.1038/461472a.

Sawyer, R.F. and Glassman, I. (1967) 'Gas-phase reactions of hydrazine with nitrogen dioxide, nitric oxide, and oxygen', *Symposium (International) on Combustion*, 11(1), pp. 861–869. Available at: https://doi.org/10.1016/S0082-0784(67)80212-1.

Sayavedra-Soto, L.A. and Arp, D.J. (2014) 'Ammonia-Oxidizing Bacteria: Their Biochemistry and Molecular Biology', in B.B. Ward, D.J. Arp, and M.G. Klotz (eds) *Nitrification*. Washington, DC, USA: ASM Press, pp. 9–37. Available at: https://doi.org/10.1128/9781555817145.ch2.

Schalk, J. *et al.* (2000) 'Involvement of a Novel Hydroxylamine Oxidoreductase in Anaerobic Ammonium Oxidation', *Biochemistry*, 39(18), pp. 5405–5412. Available at: https://doi.org/10.1021/bi992721k.

Schleper, C., Jurgens, G. and Jonuscheit, M. (2005) 'Genomic studies of uncultivated archaea', *Nature Reviews Microbiology*, 3(6), pp. 479–488. Available at: https://doi.org/10.1038/nrmicro1159.

Schmidt, I., van Spanning, R.J.M. and Jetten, M.S.M. (2004) 'Denitrification and ammonia oxidation by Nitrosomonas europaea wild-type, and NirK- and NorB-deficient mutants', *Microbiology*, 150(12), pp. 4107–4114. Available at: https://doi.org/10.1099/mic.0.27382-0.

Sedlacek, C.J. *et al.* (2020) 'Transcriptomic Response of Nitrosomonas europaea Transitioned from Ammonia- to Oxygen-Limited Steady-State Growth', *mSystems*. Edited by N. Bouskill, 5(1). Available at: https://doi.org/10.1128/mSystems.00562-19.

Shen, T. *et al.* (2013) 'Responses of the terrestrial ammonia-oxidizing archaeon *Ca* . Nitrososphaera viennensis and the ammonia-oxidizing bacterium *Nitrosospira multiformis* to nitrification inhibitors', *FEMS Microbiology Letters*, 344(2), pp. 121–129. Available at: https://doi.org/10.1111/1574-6968.12164.

Smil, V. (2001) *Feeding the world: A challenge for the twenty-first century*. MIT press.

Smith, K. (1997) 'The potential for feedback effects induced by global warming on emissions of nitrous oxide by soils', *Global Change Biology*, 3(4), pp. 327–338. Available at: https://doi.org/10.1046/j.1365-2486.1997.00100.x.

Song, H. *et al.* (2016) 'Changing roles of ammonia-oxidizing bacteria and archaea in a continuously acidifying soil caused by over-fertilization with nitrogen', *Environmental Science and Pollution Research*, 23, pp. 11964–11974.

Spang, A. *et al.* (2012) 'The genome of the ammonia-oxidizing *C andidatus* N itrososphaera gargensis: insights into metabolic versatility and environmental adaptations', *Environmental Microbiology*, 14(12), pp. 3122–3145. Available at: https://doi.org/10.1111/j.1462-2920.2012.02893.x.

Steffen, W. *et al.* (2015) 'Planetary boundaries: Guiding human development on a changing planet', *Science*, 347(6223), p. 1259855. Available at: https://doi.org/10.1126/science.1259855.

Stein, L.Y. (2011) 'Surveying N2O-Producing Pathways in Bacteria', in *Methods in Enzymology*. Elsevier, pp. 131–152. Available at: https://doi.org/10.1016/B978-0-12-381294-0.00006-7.

Stein, L.Y. (2019) 'Insights into the physiology of ammonia-oxidizing microorganisms', *Current Opinion in Chemical Biology*, 49, pp. 9–15. Available at: https://doi.org/10.1016/j.cbpa.2018.09.003.

Teske, A. *et al.* (1996) 'Distribution of sulfate-reducing bacteria in a stratified fjord (Mariager Fjord, Denmark) as evaluated by most-probable-number counts and denaturing gradient gel electrophoresis of PCR-amplified ribosomal DNA fragments', *Applied and Environmental Microbiology*, 62(4), pp. 1405–1415.

Tian, H. *et al.* (2019) 'Global soil nitrous oxide emissions since the preindustrial era estimated by an ensemble of terrestrial biosphere models: Magnitude, attribution, and uncertainty', *Global Change Biology*, 25(2), pp. 640–659. Available at: https://doi.org/10.1111/gcb.14514.

Tian, H. *et al.* (2020) 'A comprehensive quantification of global nitrous oxide sources and sinks', *Nature*, 586(7828), pp. 248–256. Available at: https://doi.org/10.1038/s41586-020-2780-0.

Treusch, A.H. *et al.* (2005) 'Novel genes for nitrite reductase and Amo-related proteins indicate a role of uncultivated mesophilic crenarchaeota in nitrogen cycling: Role of mesophilic crenarchaeota in nitrogen cycling', *Environmental Microbiology*, 7(12), pp. 1985–1995. Available at: https://doi.org/10.1111/j.1462-2920.2005.00906.x.

United Nations Environment Programme (2013) 'Drawing down N2O to protect climate and the ozone layer: a UNEP synthesis report'. Available at: https://wedocs.unep.org/20.500.11822/8489.

Venter, J.C. *et al.* (2004) 'Environmental Genome Shotgun Sequencing of the Sargasso Sea', *Science*, 304(5667), pp. 66–74. Available at: https://doi.org/10.1126/science.1093857.

Walker, C.B. *et al.* (2010) '*Nitrosopumilus maritimus* genome reveals unique mechanisms for nitrification and autotrophy in globally distributed marine crenarchaea', *Proceedings of the National Academy of Sciences*, 107(19), pp. 8818–8823. Available at: https://doi.org/10.1073/pnas.0913533107.

Winogradsky (1890) 'On the Organisms of the Nitrification', *C. R. L'Acadamie Des Science*, 110, p. 1013.

Yin, Z., Bi, X. and Xu, C. (2018) ‘Ammonia-Oxidizing Archaea (AOA) Play with Ammonia-Oxidizing Bacteria (AOB) in Nitrogen Removal from Wastewater’, *Archaea*, 2018, p. e8429145. Available at: https://doi.org/10.1155/2018/8429145.

Yu, R. *et al.* (2010) ‘Mechanisms and Specific Directionality of Autotrophic Nitrous Oxide and Nitric Oxide Generation during Transient Anoxia’, *Environmental Science & Technology*, 44(4), pp. 1313–1319. Available at: https://doi.org/10.1021/es902794a.

Yu, R. and Chandran, K. (2010) ‘Strategies of Nitrosomonas europaea 19718 to counter low dissolved oxygen and high nitrite concentrations’, *BMC Microbiology*, 10(1), p. 70. Available at: https://doi.org/10.1186/1471-2180-10-70.

Zhang, L.-M. *et al.* (2010) ‘Autotrophic ammonia oxidation by soil thaumarchaea’, *Proceedings of the National Academy of Sciences*, 107(40), pp. 17240–17245.

Zhou, X. *et al.* (2020) ‘Effects of commonly used nitrification inhibitors—dicyandiamide (DCD), 3,4-dimethylpyrazole phosphate (DMPP), and nitrapyrin—on soil nitrogen dynamics and nitrifiers in three typical paddy soils’, *Geoderma*, 380, p. 114637. Available at: https://doi.org/10.1016/j.geoderma.2020.114637.

Zhu-Barker, X. *et al.* (2015) ‘The importance of abiotic reactions for nitrous oxide production’, *Biogeochemistry*, 126(3), pp. 251–267. Available at: https://doi.org/10.1007/s10533-015-0166-4.

Zorz, J.K. *et al.* (2018) ‘Comparative Proteomics of Three Species of Ammonia-Oxidizing Bacteria’, *Frontiers in Microbiology*, 9. Available at: https://www.frontiersin.org/articles/10.3389/fmicb.2018.00938 (Accessed: 18 July 2023).